

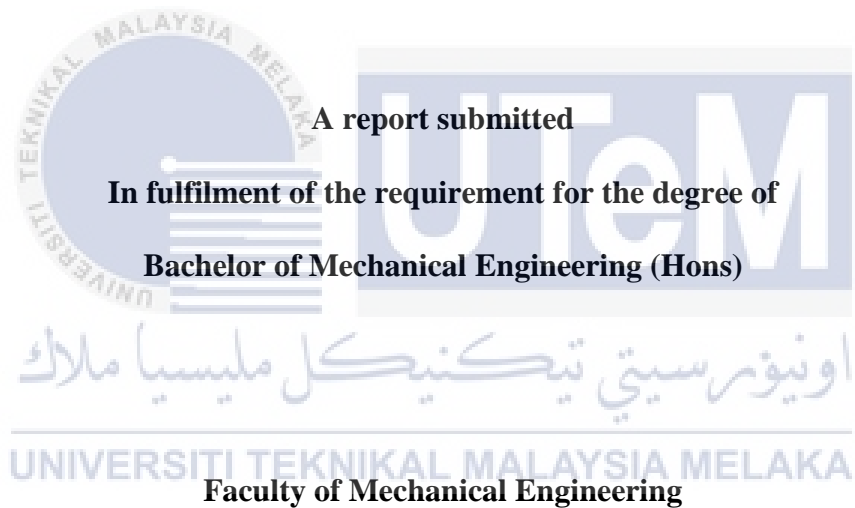
**EVALUATION OF SLIT PARAMETER OF FERROMAGNETIC  
MATERIAL BASED ON MAGNETIC FLUX LEAKAGE**



**UNIVERSITI TEKNIKAL MALAYSIA MELAKA**

**EVALUATION OF SLIT PARAMETER OF FERROMAGNETIC MATERIAL BASED  
ON MAGNETIC FLUX LEAKAGE**

**MUHAMMAD ABID MUTTAQIN BIN AMBRAN**



**UNIVERSITI TEKNIKAL MALAYSIA MELAKA**

**2020**

## DECLARATION

I declared that this project entitled “Evaluation of slit parameter of ferromagnetic material based on magnetic flux leakage” is the result of my own work except as cited in the references.

Name : MUHAMMAD ABID MUTTAQIN BIN AMBRAN

Student ID : B041610165

Date : 14<sup>th</sup> AUGUST 2020



## APPROVAL

I hereby declare that I have read this project report and in my opinion this report is sufficient in terms of scope and quality for the award of the degree of Bachelor of Mechanical Engineering.

Signature   
Name : Siti Norbaya binti Sahadan  
Date : 26<sup>th</sup> August 2020



اونيورسيتي تیکنیکل ملیسیا ملاک  
UNIVERSITI TEKNIKAL MALAYSIA MELAKA

## DEDICATION

To my beloved parents, family members and friends who have been with me throughout an  
incredible journey of this 23 years of life.



## ABSTRACT

Evaluation and testing the quality of materials are vital importance in order to maintain the productivity of materials, which could have an impact on safety and reliability of the material used. Nondestructive testing (NDT) method, which is a process of evaluating the defects on material without destroying or harming the system is used in this project due to their advantages of retaining the material's properties without causing damage. To promote the evaluation of defects on ferromagnetic materials, magnetic flux leakage (MFL) method is commonly used, which is reliable for crack detection. However, the requirement of magnetizing objects in traditional MFL method limits their applications in some condition. Hence, metal magnetic memory (MMM) method which is recently proposed by the researchers is chosen in this experiment because of their advantages of easy to operate and is more sensitive to stress. MMM method is highly effective in assessing the extent of early damages such as fatigue cracks in the ferromagnetic components because of the existence of stress concentration zone. The main purpose of this project is to evaluate the slit parameter of ferromagnetic material based on MFL. For this project, SAE 1045 carbon steel is used as the specimen due to its good machinability and offers lower cost compared to the other materials. The 3D view of the specimen models, with different slit depth and slit length are drawn by using SolidWorks software and then finite element analysis is applied to the models of the specimen. During the analysis, 100 N of tensile force is applied to the right end of the models to get the distribution of stress concentration on the models. Then, the results of stress concentration and Von Misses stress acting on the models is tabulated and graphically presented. From the results obtained, the stress concentration will increase when the slit length and slit depth increase. However, the results proved that the slit depth gives more influence to the stress concentration than the slit length. For examples at the

same length (5 mm) but with different depth, the value of the Von Mises stress increase much higher from  $1.544 \times 10^6$  N/m<sup>2</sup> to  $1.724 \times 10^6$  N/m<sup>2</sup> at 1 mm and 1.5 mm depth respectively. In contrast, at the same depth (1 mm) with different length of the slit, there are just a small increment in the value of the Von Misses stress which is from  $1.544 \times 10^6$  N/m<sup>2</sup> to  $1.555 \times 10^6$  N/m<sup>2</sup> at 5 mm and 10 mm length respectively. Then, comparative study is conducted to study and compare the results obtained from the finite element analysis with the previous study. From the comparative study, it is validated that the results of the finite element analysis are similar with the existed experimental results from previous study. Therefore, the coincidence confirms that the MFL method can be used in the evaluation of the slit parameters of ferromagnetic material.



## ABSTRAK

Penilaian dan pengujian kualiti bahan sangat penting untuk menjaga produktiviti bahan, yang dapat mempengaruhi keselamatan dan kebolehpercayaan bahan yang digunakan. Kaedah Nondestructive testing (NDT), yang merupakan proses menilai kecacatan pada bahan tanpa merosakkan atau merosakkan sistem digunakan dalam projek ini kerana kelebihan mereka mengekalkan sifat bahan tanpa menyebabkan kerosakan. Untuk mempromosikan penilaian kecacatan pada bahan feromagnetik, kaedah kebocoran fluks magnetik (MFL) biasanya digunakan, yang dapat dipercayai untuk pengesanan retakan. Walau bagaimanapun, keperluan objek magnet dalam kaedah MFL tradisional menghadkan aplikasinya dalam beberapa keadaan. Oleh itu, kaedah memori magnetik logam (MMM) yang baru-baru ini dicadangkan oleh penyelidik dipilih dalam eksperimen ini kerana kelebihanannya senang dikendalikan dan lebih sensitif terhadap tekanan. Kaedah MMM sangat berkesan dalam menilai sejauh mana kerosakan awal seperti keretakan keletihan pada komponen feromagnetik kerana adanya zon penumpuan tekanan. Tujuan utama projek ini adalah untuk menilai parameter slit dari bahan feromagnetik berdasarkan MFL. Untuk projek ini, keluli karbon SAE 1045 digunakan sebagai spesimen kerana kebolehkerjaannya yang baik dan menawarkan kos yang lebih rendah berbanding dengan bahan lain. Tampilan 3D model spesimen, dengan kedalaman celah yang berbeza dan panjang celah dilukis dengan menggunakan perisian SolidWorks dan kemudian analisis elemen hingga diterapkan pada model spesimen. Semasa analisis, daya tegangan 100 N digunakan pada hujung kanan model untuk mendapatkan taburan kepekatan tegasan pada model. Kemudian, hasil penekanan tekanan dan tekanan Von Misses yang bertindak pada model-model tersebut dijadualkan dan ditunjukkan secara grafik. Dari hasil yang diperolehi, kepekatan tekanan akan meningkat apabila panjang celah dan kedalaman celah meningkat. Walau bagaimanapun,

hasilnya membuktikan bahawa kedalaman celah memberi lebih banyak pengaruh terhadap kepekatan tegangan daripada panjang celah. Sebagai contoh pada panjang yang sama (5 mm) tetapi dengan kedalaman yang berbeza, nilai tegangan Von Mises meningkat jauh lebih tinggi dari  $1.544 \times 10^6 \text{ N / m}^2$  menjadi  $1.724 \times 10^6 \text{ N / m}^2$  pada kedalaman 1 mm dan 1.5 mm. Sebaliknya, pada kedalaman yang sama (1 mm) dengan panjang celah yang berbeza, hanya terdapat sedikit kenaikan dalam nilai tegangan Von Misses yang dari  $1,544 \times 10^6 \text{ N / m}^2$  hingga  $1,55 \times 10^6 \text{ N / m}^2$  pada 5 mm dan Panjang masing-masing 10 mm. Kemudian, kajian perbandingan dilakukan untuk mengkaji dan membandingkan hasil yang diperoleh dari analisis elemen hingga dengan kajian sebelumnya. Dari kajian perbandingan, disahkan bahawa hasil analisis elemen hingga serupa dengan hasil eksperimen yang ada dari kajian sebelumnya. Oleh itu, kebetulan mengesahkan bahawa kaedah MFL dapat digunakan dalam penilaian parameter slit dari bahan feromagnetik.



## ACKNOWLEDGEMENT

Assalamualaikum and greetings to all that involved.

First and foremost, I would like to praise and thank Allah S.W.T, whom all praise is due for His grace and goodness to give me the strength and courage to complete this final year task. Without his permission, nothing is possible.

I would like to express my sincere gratitude to my supervisor, Puan Siti Norbaya Binti Sahadan from the Faculty of Mechanical Engineering, University Teknikal Malaysia Melaka (UTeM) for the guidance and her overwhelming attitude towards the completion of this project. Her helpful comments, responses and interaction upon completing this project really helped me a lot to successfully coordinate my project. This project would not been completed without being assisted by her. I really appreciated her full cooperation and her willingness to spend her time to supervise my final year project. In a simple word, she did her responsibilities well as a supervisor.

Besides, I owe a deep sense of thanks to all supportive lecturers who have shared their knowledge and instructions from the beginning until the end. Not to forget, deepest gratitude to my parents and family for their encouragement and support for the completion of this report. Lastly, thanks to all those who contributed directly or indirectly. Their entire companion is truly appreciated as it was a great pleasure to know them. I will be grateful forever for your love. Thank You.

# TABLE OF CONTENTS

## CONTENTS

DECLARATION	i
APPROVAL	ii
DEDICATION	ii
ABSTRACT	iv
ABSTRAK	vi
ACKNOWLEDGEMENT	viii
TABLE OF CONTENTS	ix
LIST OF TABLES	xi
LIST OF FIGURES	xii
LIST OF ABBREVIATIONS	xiv
LIST OF SYMBOLS	xv
CHAPTER 1	1
INTRODUCTION	1
1.1 BACKGROUND	1
1.2 PROBLEM STATEMENT	4
1.3 OBJECTIVES	6
1.4 SCOPE OF PROJECT	6
CHAPTER 2	7
LITERATURE REVIEW	7
2.1 NONDESTRUCTIVE TESTING (NDT)	7
2.2 MAGNETIC FLUX LEAKAGE (MFL)	12
2.3 FERROMAGNETIC MATERIAL	17
2.4 CRACK PARAMETER	20
CHAPTER 3	24
METHODOLOGY	24
3.1 INTRODUCTION	24
3.2 SPECIMEN PREPARATION	29
3.2.1 MATERIAL SELECTION	31

3.3 FINITE ELEMENT ANALYSIS (FEA)	32
3.4 Comparative Study	33
CHAPTER 4	34
RESULTS AND DISCUSSIONS	34
4.1 RESULTS OF FINITE ELEMENT ANALYSIS (FEA)	34
4.2 GRAPH OF THE DISTRIBUTION OF VON MISSES STRESS.	41
4.3 COMPARATIVE STUDY	45
4.3.1 FIRST EXPERIMENT	45
4.3.2 SECOND EXPERIMENT	52
4.3.3 THIRD EXPERIMENT	57
4.3.4 FOURTH EXPERIMENT	64
4.3.5 FIFTH EXPERIMENT	75
CHAPTER 5	81
CONCLUSION AND RECOMMENDATIONS	81
5.1 CONCLUSION	81
5.2 RECOMMENDATIONS FOR FUTURE WORKS	82
REFERENCES	83



## LIST OF TABLES

Table 2. 1 : Commonly used nondestructive testing method. ....	9
Table 2. 2 : Comparison between NDT and destructive testing.....	11
Table 2. 3 : Curie temperature of materials.....	19
Table 3. 1 : Gantt chart for PSM 1 .....	26
Table 3. 2 : Gantt chart for PSM 2 .....	27
Table 3. 3 : Slit parameters of specimen. ....	30
Table 3. 4 : Chemical composition of SAE 1045 carbon steel.....	31
Table 4. 1 : Values of maximum Von Misses stress for different size of slit. ....	43
Table 4. 2 : Values of defect depth.....	49
Table 4. 3 : values of defect location.....	51
Table 4. 4 : Physical properties of the material. ....	54
Table 4. 5 : Components of the material. ....	54
Table 4. 6 : Features of experiment setup.....	71
Table 4. 7 : Programmed load spectrum.....	72
Table 4. 8 : Comparison between the sensor's results and the analysis of fracture. ....	74
Table 4. 9 : Simulations parameters for MMM simulations.....	77

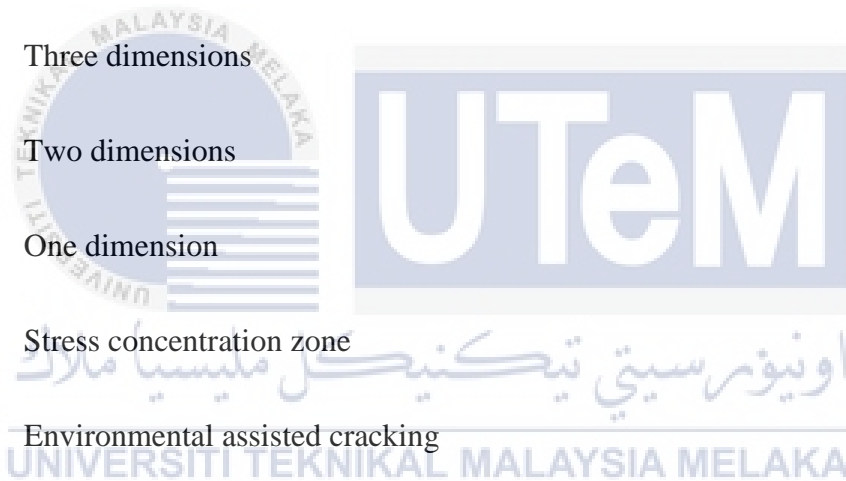
## LIST OF FIGURES

Figure 2. 1 : Dye penetrant testing. ....	8
Figure 2. 2 : Magnetic field leakage. ....	13
Figure 2. 3 : Distribution of tangential and normal component of SMFL. ....	15
Figure 2. 4 : Orientation of the magnetic domain, where M is magnetic domain. ....	18
Figure 2. 5 : Longitudinal crack in weld material. ....	21
Figure 2. 6 : Crack profile in pipeline steel. ....	23
Figure 3. 1 : Overall flow of the experiment. ....	25
Figure 3. 2 : Design model of specimen. ....	29
Figure 3. 3 : Specimen with 100 N applied force. ....	32
Figure 4. 1 : Drawing of the specimen by using SolidWorks. ....	35
Figure 4. 2 : Specimen with fixed geometry and applied force. ....	36
Figure 4. 3 : Meshed specimen model with 50% of mesh density. ....	37
Figure 4. 4 : Von Mises stress distribution of the plate with 3 mm length at different depth (a)0.5 mm (b)1.0 mm (c)1.5 mm. ....	38
Figure 4. 5 : Von Mises stress distribution of the plate with 5mm length at different depth (a)0.5 mm (b)1.0 mm (c)1.5 mm. ....	39
Figure 4. 6 : Von Mises stress distribution of the plate with 10 mm length at different depth. ....	40
Figure 4. 7 : Graph Von Mises stress vs slit length at 0.5 mm, 1.0 mm and 1.5 mm depth. ....	41
Figure 4. 8 : Graph Von Mises stress vs depth at 3 mm, 5 mm and 10 mm slit length. ....	42
Figure 4. 9 : Schematic view of SMFL distribution in the stress concentration zone. ....	46
Figure 4. 10 : Distribution of normalized tangential and normal component along the x-axis direction. ....	47
Figure 4. 11 : SMFL signal versus defect depth : (a) tangential component and (b) normal component. ....	48
Figure 4. 12 : Influence of defect depth on the normalized SMFL amplitudes : ....	48
Figure 4. 13 : SMFL signal versus w (Y=0.5 mm, b=3 mm, d=2 mm) : (a) tangential component and (b) normal component. ....	50
Figure 4. 14 : Influence of w on the normalized SMFL amplitudes : ....	50
Figure 4. 15 : Experimental system : ....	52
Figure 4. 16 : Specimen dimension and scanning line. ....	53
Figure 4. 17 : The distribution of stress on the scanning line. ....	53
Figure 4. 18 : Magnetic distribution perpendicular to the surface of specimens. ....	55
Figure 4. 19 : Magnetic abnormality caused by different level of stress concentration on the scanning line : (a) with a tension of 800 N, (b) with a tension of 2000 N. ....	56
Figure 4. 20 : Pipelines subjected to internal pressure. ....	58
Figure 4. 21 : Schematic of specimen with the thickness of 5 mm. ....	58
Figure 4. 22 : Finite elements model of the specimen and the surrounding air region. ....	59
Figure 4. 23 : Von Mises equivalent stress for the specimen under tensile load (12.7 kN). ....	59
Figure 4. 24 : The MFL simulation results along different measuring lines under tensile load (12.7 kN). ....	60
Figure 4. 25 : MFL differences before and after loading (measuring line 4). ....	61

Figure 4. 26 : MFL differences before and after loading (measuring line 3).	61
Figure 4. 27 : MFL differences between two tensile loads of 24.7 kN and 12.7 kN.	63
Figure 4. 28 : Geometry of the sensor and washer.	65
Figure 4. 29 : schematic view of monitoring process.	66
Figure 4. 30 : Smart washer.	67
Figure 4. 31 : Finite element model.	68
Figure 4. 32 : Results of finite element analysis.	68
Figure 4. 33 : The maximum stress and deformation with the radius of the washer.	69
Figure 4. 34 : Experiment setup.	70
Figure 4. 35 : Self-developed monitoring software.	70
Figure 4. 36 : Changes of signals from top sensor.	73
Figure 4. 37 : Changes of signal sampled by the sensor (aqueous solution).	74
Figure 4. 38 : Schematic representation of MMM signals due to stress concentration zone.	75
Figure 4. 39 : Magnetic charge models for the local stress concentration.	76
Figure 4. 40 : Comparison of axial component of MMM signals between experimental data and theoretical models.	77
Figure 4. 41 : MMM signals simulation for a specimen with 3D stress-concentration zone.	78
Figure 4. 42 : Distribution of normal component of MMM signals with the change in length, depth, width and lift-off values.	79
Figure 4. 43 : Specimen with a long elliptical defect.	80
Figure 4. 44 : (a) Stress distribution in the z direction. (b) Stress distribution in the x direction.	80

## LIST OF ABBREVIATIONS

NDT	-	Nondestructive testing
MFL	-	Magnetic flux leakage
MMM	-	Metal magnetic memory
AC	-	Alternating current
DT	-	Destructive testing
SMFL	-	Self-magnetic flux leakage
3D	-	Three dimensions
2D	-	Two dimensions
1D	-	One dimension
SCZ	-	Stress concentration zone
EAC	-	Environmental assisted cracking
FEA	-	Finite element analysis
FEM	-	Finite element method



## LIST OF SYMBOLS

$q$	-	Internal pressure
$H_{p(x)}$	-	Tangential SMFL component
$H_{p(y)}$	-	Normal SMFL component
$\sigma_{\theta}$	-	Circumferential tension stress
$\sigma$	-	Stress
$w$	-	Defect location
$y$	-	Lift-off value
$b$	-	Width
$d$	-	Depth
$f$	-	Frequency
$R$	-	Stress ratio
$C$	-	Carbon
$Mn$	-	Manganese
$Cr$	-	Chromium
$Si$	-	Silicon
$p$	-	Phosphorus
$Ni$	-	Nickel



- Mo - Molybdenum
- Cu - Copper
- M - Magnetic domain



# CHAPTER 1

## INTRODUCTION

### 1.1 BACKGROUND

Ferromagnetic materials are strongly magnetized when subjected to the external magnetic field and retain its magnetic moment even when the applied field is removed. Ferromagnetic materials do not only respond strongly to magnets, but they can also be magnetized, attracted to magnets and form permanent magnets. Ferromagnetism is the spontaneous magnetization phenomenon that exists in the ferromagnetic material in the absence of applied magnetic field. The examples of the ferromagnetic materials are transition metals such as ferum, nickel and cobalt (Wang et. al, 2013).

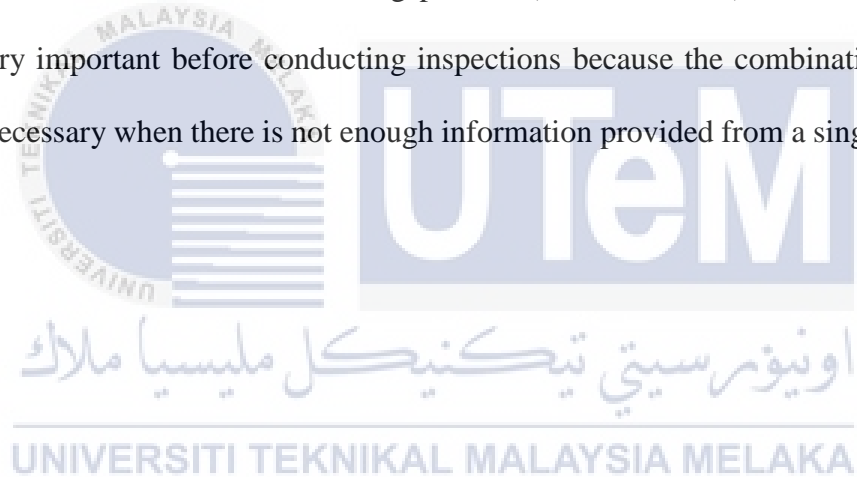
Nondestructive testing (NDT) is used during this project rather than destructive test because of their advantages that retain the properties of materials without causing damage. NDT is the process of evaluating and testing the defects of materials without destroying or harming the system. In other words, the part can still be used after it was tested (Gupta, 2018).however, destructive testing are destructive in nature and are conducted on the limited sample, rather than on the materials (Dwivedi, 2017). The traditional method of inspecting the quality of materials have several disadvantages such as results are not predicted immediately and destructive in nature. In addition, the traditional method which is destructive testing, are usually not appropriate for parts in operation. Therefore, several NDT methods have been developed to overcome the limitations.

Nowadays with the grows in technology, NDT is commonly applied in manufacturing and piping to inspect the materials and products integrity and reliability and to maintain the

quality of materials (Usarek et. al, 2017). These methods have been drawn more attention due to the reliability and effectiveness of the testing process (Verma et. al, 2013). Eddy current, ultrasonic and magnetic flux leakage are among the types of NDT method that are commonly used for defect investigation. Eddy currents are generated by an electromagnetic induction system. Eddy currents testing is commonly used for the inspection of various type of defects such as surface crack detection, to measure the coating thickness and the determination of depth (Dwivedi, 2017). Ultrasonic technique is used to inspect or evaluate the internal flaws in sound-conducting materials, while the magnetic flux leakage is the most popular NDT method which uses a sensitive magnetic signal. Magnetic flux leakage (MFL) is used to detect crack, where the induced magnetic field will change with the existence of cracks in the specimen. This method of testing can measure the distribution of the magnetic field on the magnetized specimen and therefore has been applied in evaluating defects on specimens (Shi, 2015).

Crack is a major concern in ensuring the durability, safety and serviceability of structures. This is because the presence of crack can cause the reduction in the effective loading area which lead to the increase of stress and subsequently failure of the materials or structures. Cracking seems unavoidable and appears in wide variety of structures such as concrete wall, beam and brick walls. Various types of defects also can be found in pipeline applications (Agbainor, 2014). Slit and crack are the examples of defects that commonly found especially in the ferromagnetic materials. The presence of defects will affect the reliability, safety and the consistency of materials' quality. Therefore, it is crucial to test and evaluate the materials or structure to detect cracking for the safety and health of the structure. The presence of such cracks can be detected by using various types of NDT.

However, these methods or techniques have their own advantages and limitations depends on their use and applications (Gholizadeh, 2016). NDT plays a vital role to identify the existence of defects that enables the early planning for the structure replacement from the results of testing or evaluation (Verma et. al, 2013). Combination of different NDT is a good way to inspect the defect and abnormalities of the structures. In many cases, more than one NDT method is use in the process of defect inspection. To ensure the effectiveness of the inspection process, more understanding on the backgrounds, advantages and limitations of each NDT technique is necessary. Understanding one nondestructive method alone may not be enough to obtain the accurate results from the testing process (Dwivedi, 2018). Therefore, analysis of signals is very important before conducting inspections because the combination of different methods is necessary when there is not enough information provided from a single test method.



## 1.2 PROBLEM STATEMENT

Evaluation and testing the quality of material are very important during the life of a material (Verma, 2013). To maintain the productivity of the materials, proper inspection techniques are required for infrastructure deterioration. NDT is an important method for the inspection of surface and subsurface flaws which could have an impact on safety and reliability of the material used. The issue of inspection is important especially during the production stages. Factors such as economics, safety and the use of constructive designs come into play when product quality is of concern.

Based on the recent studies, there are various type of defect that could affect the productivity of materials. The purposed of this project is to characterize the slit parameter of ferromagnetic material based on MFL. Slit and crack are the examples of defects that commonly found in the ferromagnetic materials. The presence of these types of defects will give an impact to the consistency of the materials quality and directly will affect the reliability and safety of materials. For a better understanding, crack is either a stress corrosion crack or a fatigue crack which is artificially produced or formed naturally. In other hand, defect is commonly used to refer a crack, slit or other abnormalities such as corrosion (Yusa, 2009).

With the current development in technology, there are many types of NDT method that available to detect crack. Liquid penetrant testing is one of the basic methods which can be used for defects or cracks detection. During this method of testing, liquid dye penetrant is applied to the material surface and then drawn into any surface with cracks or slits, highlighting the detected cracks on the materials. Other than that, eddy current testing is capable in detection of surface crack. Eddy current testing utilizing low frequency of electromagnetic fields which induces eddy currents

inside the test materials. This method with high speed and sensitivity of inspection for surface cracks offers a suitable inspection method especially for surface cracks (Yusa, 2009). However, this method is basically used for conductive materials and more difficult to determine the defects that embedded in the specimen. Theoretically, phase measured signal can be used to characterize the defect depth. However, it is complicated to evaluate the phase of signals in reality (Yusa, 2010).

Therefore, instead of using eddy current to characterize the slit parameter of ferromagnetic material, it is more preferable to use metal magnetic memory (MMM) due to the numbers of significant advantages compared to other methods for the inspection of ferromagnetic materials (Wang, 2009). MMM is a newly developed NDT method which is capable to detect early failure such as fatigue damage, micro crack and stress concentration of material. One of the advantages of MMM method is that the model does not require special magnetizing equipment as the magnetization unit phenomenon is used in this operation. Other than that, this method with small-sized instruments will ease the inspection and testing process, besides having self-contained power supply (Ning, 2017).

### 1.3 OBJECTIVES

The objectives of this project are :

- 1.3.1 To characterize the slit parameter of ferromagnetic material based on magnetic flux leakage.
- 1.3.2 To study the distribution of stress concentration based on different approaches.
- 1.3.3 To validate the MMM method with different methods of NDT.



### 1.4 SCOPE OF PROJECT

The scopes of the project are:

اونيورسيتي تیکنیکل ملیسيا ملاک

UNIVERSITI TEKNIKAL MALAYSIA MELAKA

- 1.4.1 This study is conducted by using FEA.
- 1.4.2 The sample of this project is made of SAE 1045 carbon steel.
- 1.4.3 Crack imitation (slit) is used in this project, rather than the actual crack.

## CHAPTER 2

### LITERATURE REVIEW

#### 2.1 NONDESTRUCTIVE TESTING (NDT)

NDT is the analysis technique used to evaluate, inspect and test the serviceability of the system without damaging the system. Its effectiveness in evaluating material quality for surface and internal flaws or metallurgic condition without destruction of the material has drawn more and more attention (Verma, 2013). This technique is a highly valuable and recommended technique to determine the quality of materials or systems that can save both time and money in materials evaluation (Louis, 1995).

Nowadays with the development of NDT method, this testing method is utilized in numbers of applications which covers variety of industrial activity. These methods are used in the application of manufacturing, piping and in-service inspection for the product integrity and reliability and to maintain a uniform quality level of the materials (Usarek, 2017). In addition, it can prevent the materials failure that would cause significant hazard especially in building structures and piping. There are various type of NDT technique available for the inspection or testing process such as MFL, eddy current, ultrasonic test and dye penetrant test. The example visualization of crack from dye penetrant test is shown in Figure 2.1.

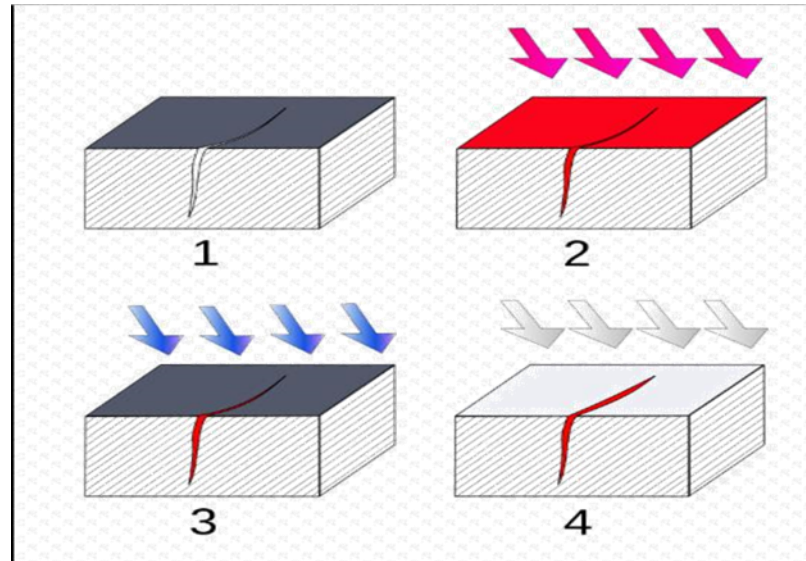


Figure 2. 1 : Dye penetrant testing.

( Source : 2006, Retrieved November 11 2019

[https://commons.wikimedia.org/wiki/File:Ressuage\\_principe\\_2.svg](https://commons.wikimedia.org/wiki/File:Ressuage_principe_2.svg) )

The figure above shows the simple process of dye penetrant testing. At the beginning of the process, the surface-breaking crack of the material is not visible to the naked eye. Liquid dye penetrant is applied to the surface and the developer is applied, rendering the crack visible. Eddy current testing is among the commonly used NDT which enables crack detection in various types of conductive materials, either non-ferromagnetic or ferromagnetic. This method of testing can be applied without directly put in contact the sensor and the materials that is under test.

NDT methods can be used for the inspection of many types of materials such as metals, plastics, ceramics and composites to determine the existence of crack, surface cavities and any

type of defect that will cause the systems failure (Dwivedi, 2018). Commonly used NDT methods are shown in Table 2.1.

Table 2. 1 : Commonly used nondestructive testing method.

<b>Technique</b>	<b>Capabilities</b>	<b>Limitations</b>
Visual inspection	Macroscopic surface defects.	Difficult to inspect small defects, no subsurface defects.
Magnetic flux leakage (MFL)	Detection and sizing of corrosion pits in ferrous plates and pipes.	Very poor in detecting of axial cracks.
Ultrasonic	Subsurface defects	Material need to be sound-conducting material.
Eddy current	Surface and near surface defects.	Complicated to applied in certain application; only for metals.
Dye penetrate	Subsurface defects	Cannot normally applied to painted materials.

These variety of testing methods ensure the inspection and testing process become more efficient. However, these methods or techniques have their own advantages and limitations depends on their use and applications. To counter this problem, more than one NDT methods can be applied to detect the defect. In many cases, combination of different NDT methods available is used rather than using a single method in order to minimize those effects (Gholizadeh, 2016). Therefore, more understanding related to the backgrounds, advantages and limitations of each

NDT technique is necessary to ensure the effectiveness of the inspection process. Analysis of signals is very important before conducting the inspection process because the understanding of one NDT method alone is insufficient to ensure the effectiveness of the inspection process. Thus, a sufficient knowledge about NDT is needed before choosing the appropriate method of analysis to ensure a better performance of NDT (Verma, 2013).

Other than NDT, the tests are destructive in nature which are conducted on the limited number of sample rather than on the materials. These destructive testing are usually used to test the physical properties of materials such as ductility, fatigue strength, and fracture toughness. These tests are generally provide more information and easier to analyze than NDT. However, characterization of differences and discontinuities in the characteristics of material can be more accurate and effective by using NDT. Generally, destructive test is not convenient to apply to parts in service because it requires the interruption of service or system operation and the parts are permanently removed from the service (Aire, 2016). The differences of nondestructive testing and destructive testing are as shown in Table 2.2.

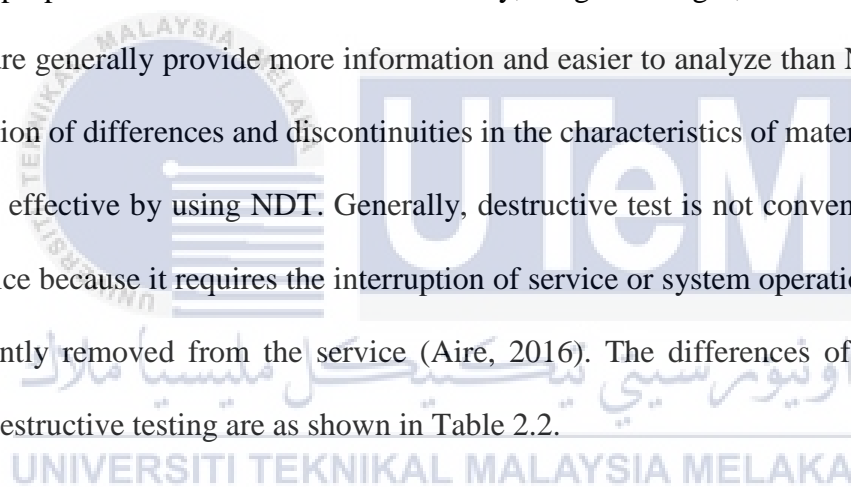


Table 2. 2 : Comparison between NDT and destructive testing.

<b>Nondestructive testing (NDT)</b>	<b>Destructive testing</b>
To determine the defects of materials.	To determine the materials properties.
Load is not applied on the materials.	Load is applied on the materials.
No materials damage due to no load applications.	Materials get damage due to load application.
Examples: ultrasonic testing, dye penetrant test, MFL.	Examples: tensile test, compression test, hardness test.

## 2.2 MAGNETIC FLUX LEAKAGE (MFL)

MFL is one of the NDT methods that commonly used in materials testing and analysis to detect corrosion and pitting in steel structures, especially for defects in pipelines and storage tanks applications. This technique was early introduced to the pipeline inspection since 1960s. In the early stage, magnetic powder was used which displayed the defects by piling up. Nowadays with the development of the technology, magnetic sensor is used for the inspection process which ensures the process is conducted effectively.

Pipeline system is widely used in oil industry as it is the most effective way to transport the oil and gas. However, this system which buried the pipelines underground will easily affected by the pressure and humidity which can lead the pipelines to some defects such as corrosion and deformation (Shi, 2015). Therefore, it is important to use a convenient testing method to detect various types of pipeline failures that usually caused by corrosion and external agents. These failures will contribute to pipeline leaking and rupture that will negatively affect the natural environment, infrastructure and economy. Thus, it is vital to carry out the evaluation of the system to prevent such problems (Ruiz, 2015). Moreover, this kind of testing method with several benefits compared to other NDT method is convenient to be used in the inspection of pipeline abnormalities and defect. High-speed inspection, good sensitivity to pitting and can be used in all ferromagnetic materials are among the benefits of using MFL testing method. By using this method, it will be helpful for early identification of the area of failure to ensure the safety of the operation or system.

MFL method uses powerful magnet to magnetize the material that is under test. The magnetic field will leak from the material where there are internal or external metal loss once

the sensor detects the defects or abnormalities. The magnetic field will remain undisturbed if the material under tests has no flaws. This will help to identify the specific area which need to have some preventative maintenance or to be repaired. Moreover, magnetic flux leakage testing technology is not only can be used in defect detection, but can also be used in analyzing the characteristic of the defects. The magnetic field leakage once the internal and external defects are detected is shown in Figure 2.2.

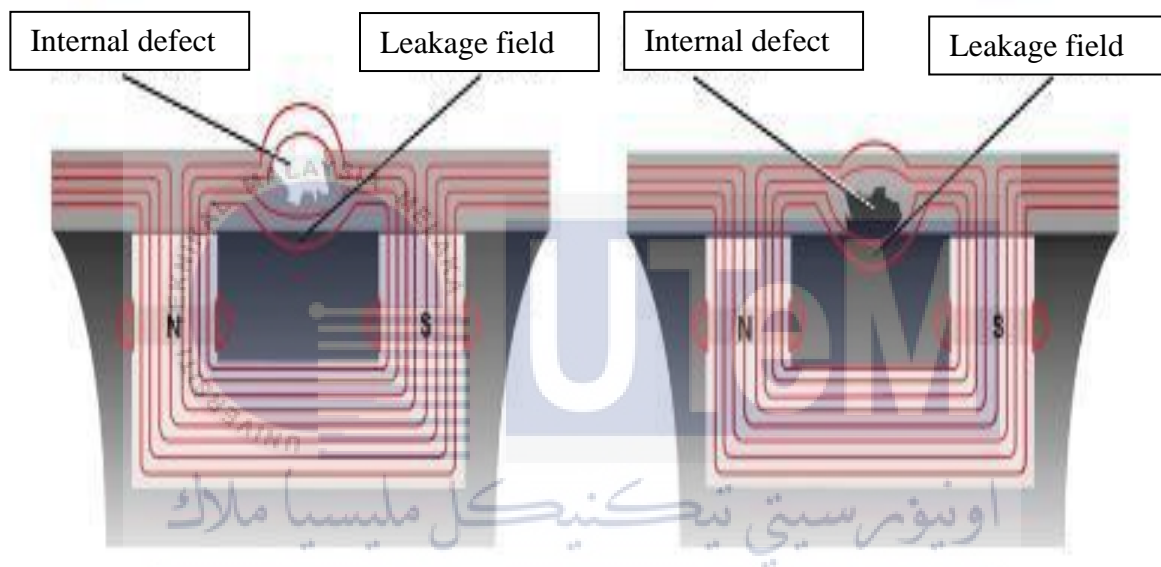


Figure 2. 2 : Magnetic field leakage.

(Source : 2019, Retrieved November 22 2019

<https://www.rosen-group.com/global/company/explore/we-can/technologies/measurement/mfl.html> )

MFL testing method has become a pivotal function for pipeline inspection process due to its advantages rather than other NDT method. However, this method has its own limitations. In this method of testing, the main point is how to analyze the type of defects from the measured magnetic flux signals. Width, depth and the location of the defect are used to characterize the defect that is detected from the leakage of the magnetic field. However, it is complicated to

specify each of the parameters from the measured MFL. Moreover, elastic and plastic zone nearby to the cracks is also one of the obstacles in conducting this method. Idealized material properties are generally assumed due to no detail knowledge of the effects of plastic deformation on the magnetic properties of ferromagnetic material (Wang, 2012).

With the recent development of magnetic flux leakage, MMM is a newly developed NDT that enable the detection of early defects such as micro-crack, stress concentration and fatigue damage of materials. This technique provide a great impact in testing and inspection process and been investigated over the years. Other traditional methods likes ultrasonic testing, magnetic particle inspection and x-ray are commonly used to detect the already developed defects such as crack and corrosion. Thus, by using those methods, sudden fatigue damages which can cause failures and directly can cause the hazard will not be identified. This fatigue damage that occurred at the stress concentration zone, are mainly the major sources of damages that occurred in operating system due to the intensive development of corrosion, fatigue and creep processes. Stress concentration zone of ferromagnetic material can be detected by using MMM method because the state of the magnetic is retained even when the removal of the load. The residual lifetime of ferromagnetic materials also can be predicted by using this method. In facts that this method is a newly developed testing method, this weak magnetic test method with insufficient knowledge and various kind of disturbance factors during testing process will limit the mechanism and quantitative detection of this method. Thus, this method is only used as a preliminary qualitative testing method to identify the defects and abnormalities of the materials (Bao, 2016).

MMM is a method that can detect the early defect of a ferromagnetic material by monitoring the distribution of self-magnetic flux leakage (SMFL) signals. These signals consist of normal and tangential component which are perpendicular and parallel to the surface of specimen, respectively. Previously, numbers of studies have confirmed that the distribution of SMFL signal are affected by the applied stress. However, the variations of the SMFL signal of MMM which is known as a weak magnetic testing method, could be influenced by the other factors such as external load, chemical composition of materials and the depth and location of the defect. These factors could give certain impact on the intensity of the SMFL field, where the significant influence on its distribution characteristic has not been found (Bao, 2016). Figure 2.3 shows the schematic of SMFL distribution in the stress concentration zone.

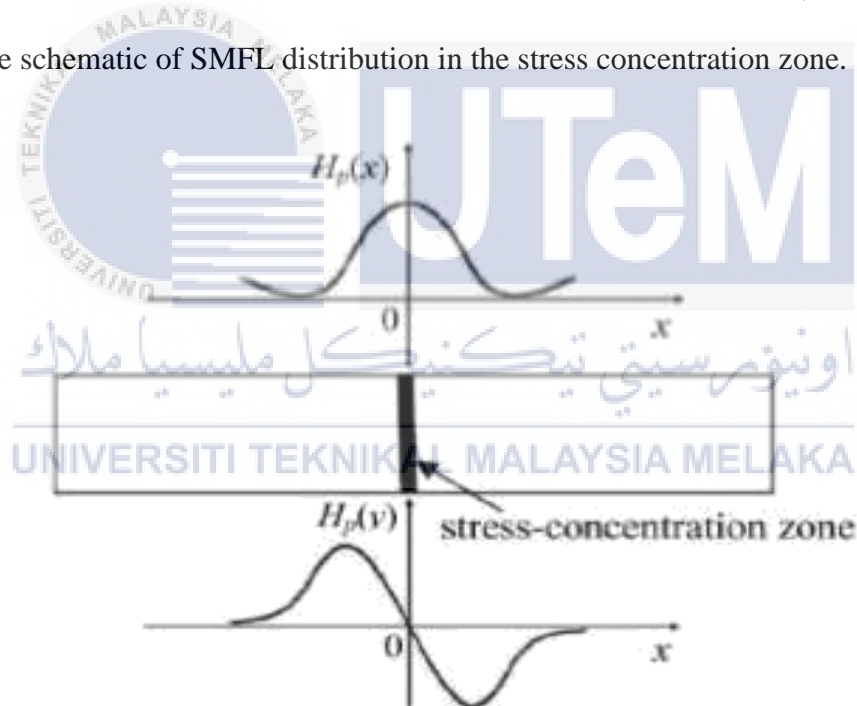


Figure 2. 3 : Distribution of tangential and normal component of SMFL.

(Source : Bao, 2016)

MMM method is commonly used in various applications such as in oil and gas industries, power engineering, aviation and chemical industry due to numbers of significant advantages

compared to the other methods. Application of this method uses the phenomenon of its equipment and structures unit magnetization in the inspection process. This facility simply will ease the inspection process without the requirement of special magnetizing devices likes the other nondestructive testing methods. Moreover, this method is easier to conduct due to the small size of instruments used and self-contained power supply. The materials or components can be directly tested because of early preparation of the test surface such as metal dressing is not required before conducting the inspection process. Thus, the cost required for the inspection process can be reduced.



## 2.3 FERROMAGNETIC MATERIAL

Ferromagnetic material is a material which can attract to magnets and become permanent magnets. Ferromagnetic materials do not only respond strongly to magnets, they can also magnetize themselves. A bulk piece of ferromagnetic material consists of regions which are called magnetic domain. Magnetic domain is actually a tiny region in ferromagnetic material which have their own specific overall spin orientation that is caused by quantum mechanical effect. When some unpaired electrons are considered, the electrons will exchange interaction with each other and they will line up themselves in a tiny region based on the direction of the magnetic field (Kiefer, 2005).

Magnetic domains in a material are the regions of spontaneous alignment of electron spins due to their magnetic field, which can be altered by the external magnetic field applied to the material. The magnetic domains tend to reorient into the same direction as the direction of the applied magnetic field when subjected to the external magnetic field. The domains will retain in the same direction with external magnetic field even when the removal of the field, thus creating a permanent magnet. This behavior cause the domain walls tend to become pinned on defects in the crystal lattice, maintaining the parallel orientation. However, the domain walls tend to move back to a minimum energy configuration with reducing external magnetic field by heating and cooling or by hammering the material, thus demagnetizing the material. The orientation of the magnetic domains before and after magnetization occurs is shown in Figure 2.4.

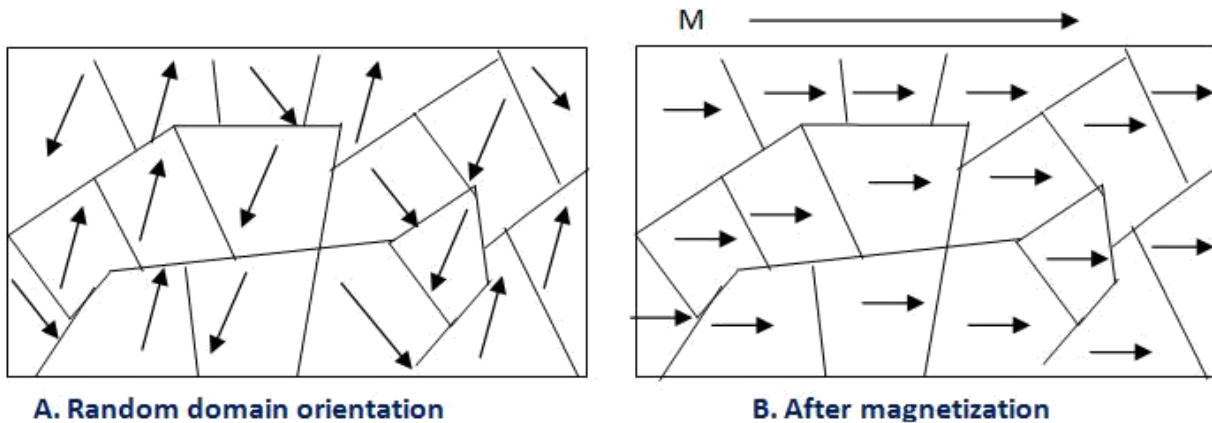


Figure 2. 4 : Orientation of the magnetic domain, where M is magnetic domain.

(Source : 2019, Retrieved November 25 2019

<https://www.yourelectricalguide.com/2017/05/hysteresis-loop-hysteresis-loss.html> )

This behavior of ferromagnetic material is called ferromagnetism which the material becomes a permanent magnet by the applied magnetic field. Ferromagnetic materials can be easily magnetized and the magnetization approaches a definite limit called saturation in strong magnetic field. The common ferromagnetic materials are cobalt, iron, nickel and most of their alloy. Ferromagnetism is vital in modern industry and technology as it is fundamental for many electromechanical and electrical system such as generators, transformers and nondestructive testing of ferrous materials (Gao, 2008).

As stated before, ferromagnetic materials are widely used in many types of devices in daily life due to some benefits. Ferromagnetic materials, which have high residual magnetism and high coercivity assure that they are the ideal material that used to form permanent magnet. However, ferromagnetic materials could not maintain a spontaneous magnetization once the temperature reach a point called Curie temperature. Thus, the ability of the materials to be magnetized disappears although it stills can paramagnetically responds to the external field. At

Curie temperature, ferromagnetic material becomes paramagnetic material where the ferromagnetic materials will lose their magnetic properties. This occurs because the higher temperature provides sufficient thermal energy for the material to overcome the internal aligning forces of the material (Mohn, 1987). Paramagnetic materials do not retain the magnetic properties when the removal of the external field and are slightly attracted by the magnetic field. These paramagnetic materials have a small susceptibility to magnetic field. Curie temperature of some materials are shown in Table 2. 3.

Table 2. 3 : Curie temperature of materials.

Material	Curie Temperature in Kelvin
Ferum	1043
Nickel	627
Cobalt	1388

UNIVERSITI TEKNIKAL MALAYSIA MELAKA

## 2.4 CRACK PARAMETER

Crack is simply a material failure that can be easily understood as material or component breakdown without complete separation of its adjoining parts. For a safe structure, it is important for the early detection of a crack to prevent or eliminate various types of cracks. Without any approach of the cracks, the propagation of such cracks can finally result in fracture and may lead to systems collapse. Areas with low shear and high bending stresses usually have flexural cracks. Those bending and shear stresses are the main causes for the propagation of cracks which lead to the material failure (Sharma, 2014).

Crack is generally a defects or flaws which caused by material deformation that appear on the material. The external forces subjected to the material will generate deformation that can cause cracking. Compressive crack and tensile crack are parallel and perpendicular to the applied force, respectively (He, 2019). In many applications, crack is also found in welded material. Crack in welding depends on many factors such as type of material, the welding environment and the welding process itself. This type of crack is due to the thermal stresses that is induced from the welding process (Yusof, 2014). Figure 2.5 shows the longitudinal crack which is commonly occurred in weld material.

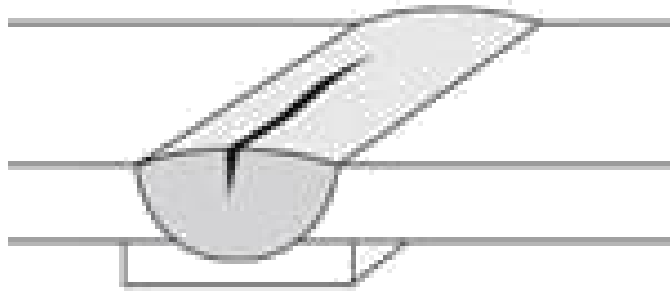


Figure 2. 5 : Longitudinal crack in weld material.

(Source : 2014, Retrieved November 25 2019

<http://weldinganswers.com/why-welds-crack/>)

The presence of the defects as shown in Figure 2.5 will give negative impact on the material and directly will interrupt the effectiveness of the material or system. Moreover, defects of material could be more dangerous that can cause loss of life, economic loss and also will affect the loss of products or services. Therefore, it is vital to make an approach in detecting cracks in order to minimize and eliminate the presence of cracks in material. NDT is the potential technique that commonly used to detect the presence of those dangerous cracks.

In industries, crack may occur during manufacturing, testing or use because it is impossible to produce product which is totally immune to crack. Crack is simply defined as material break or rupture without complete separation of parts which generally occurs with a sudden sound. The products are usually subjected to fatigue loading which can lead to material crack due to cyclic loading. These kinds of cracks will lead to manufacturing failure which occur in different materials such as metal, composite, plastics and minerals. However, time to time checking of the material during the production or manufacturing process will help to minimize the occurrence of the crack. Inadequate crack detection and analysis may lead to various hazards that can cost human life. The ability to detect cracks that are caused by fatigue, thermal shocks and stress corrosion is

important to ensure safety of materials and components. For example, many incidents that occur in nuclear fuel rod in nuclear reactor which is the main safety barrier of the system are due to the cracks and ruptures in these parts. In addition, crack can lead to the early initiation of corrosion in steel because it provides easy access to the ingress of chlorides that can cause corrosion. Apart from that, the width, length and cracking frequency of the crack are all can influence the corrosion of the steel. The formation of cracks will adversely affect its durability properties. (Shaikh, 2018).

Cracks can occur in any materials such as composites, plastics, metals and minerals that can lead to major failures in industries such as in automotive, aerospace and building. Cracks are commonly found in wide variety of application especially in piping application. Cracking on the internal and external surfaces of in-service pipes and tanks reduces the integrity of the material and will reduce the lifetime of the equipment. In pipelines application, stress corrosion cracking is one of the types of crack that is commonly found. Environment of the pipeline application itself can contribute to the presence of an initial corrosion area that is acted on by stresses that result in the growth of crack. This initial corrosion area is due to the contact between water and steel of the pipe. Residual stress, load stress and local stress are among the factor that cause the crack growth. Other than that, crack characteristics are generally depend on the cause of the crack, the materials being cracked and the environments that cause the crack (Ginzel, 2002). Figure 2.6 shows the crack profile in pipeline steel.

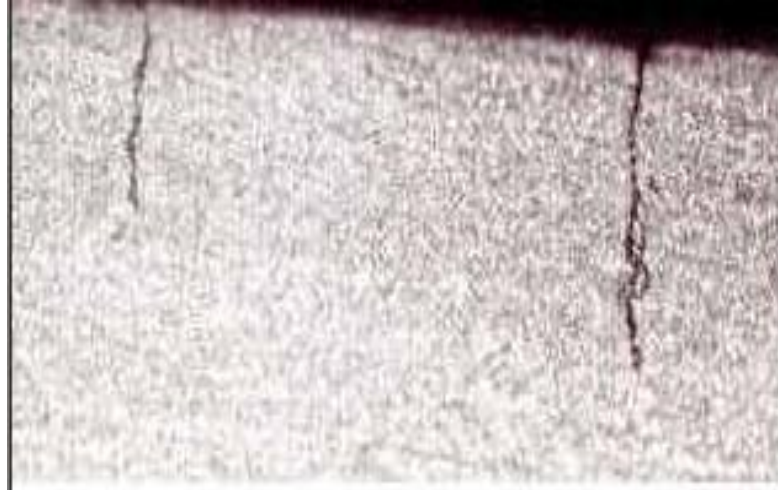


Figure 2. 6 : Crack profile in pipeline steel.

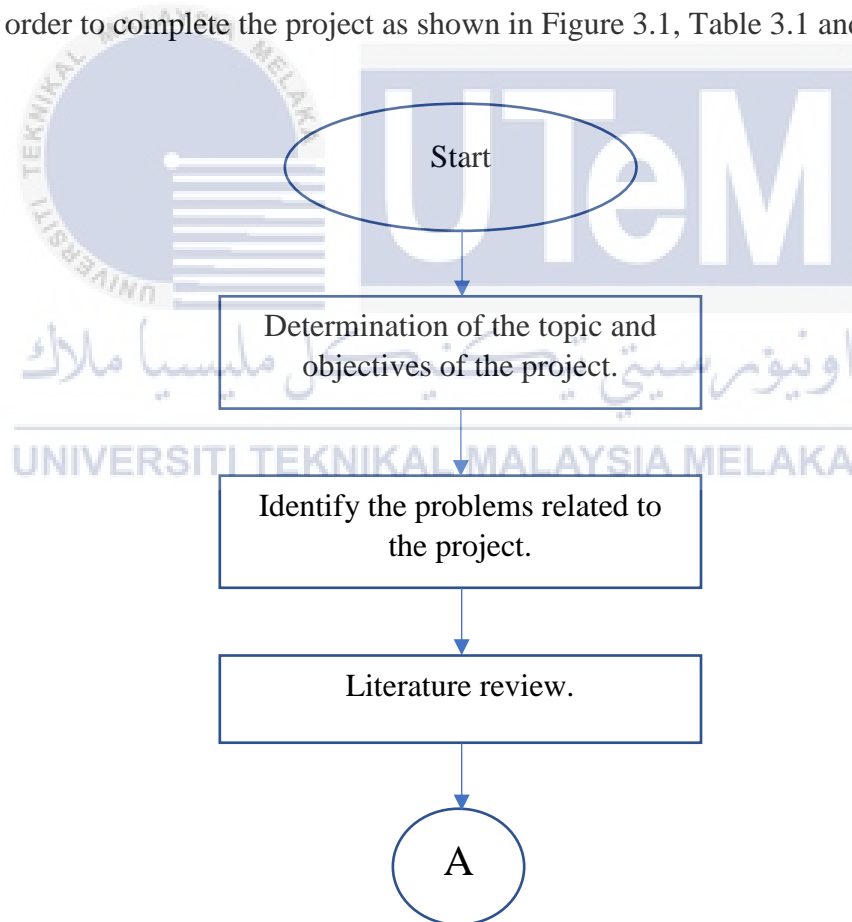


## CHAPTER 3

### METHODOLOGY

#### 3.1 INTRODUCTION

This chapter will explain the methodology that is being used to ensure this project is well completed. It compasses tools and techniques to conduct a particular research or finding. While conducting this project, it is vital to select an accurate and proper method that suits the project objective to collect all the necessary information. In order to identify all the information and data, planning must be done in the proper manner. Overall operational flow of the project is to illustrate the order to complete the project as shown in Figure 3.1, Table 3.1 and Table 3.2.



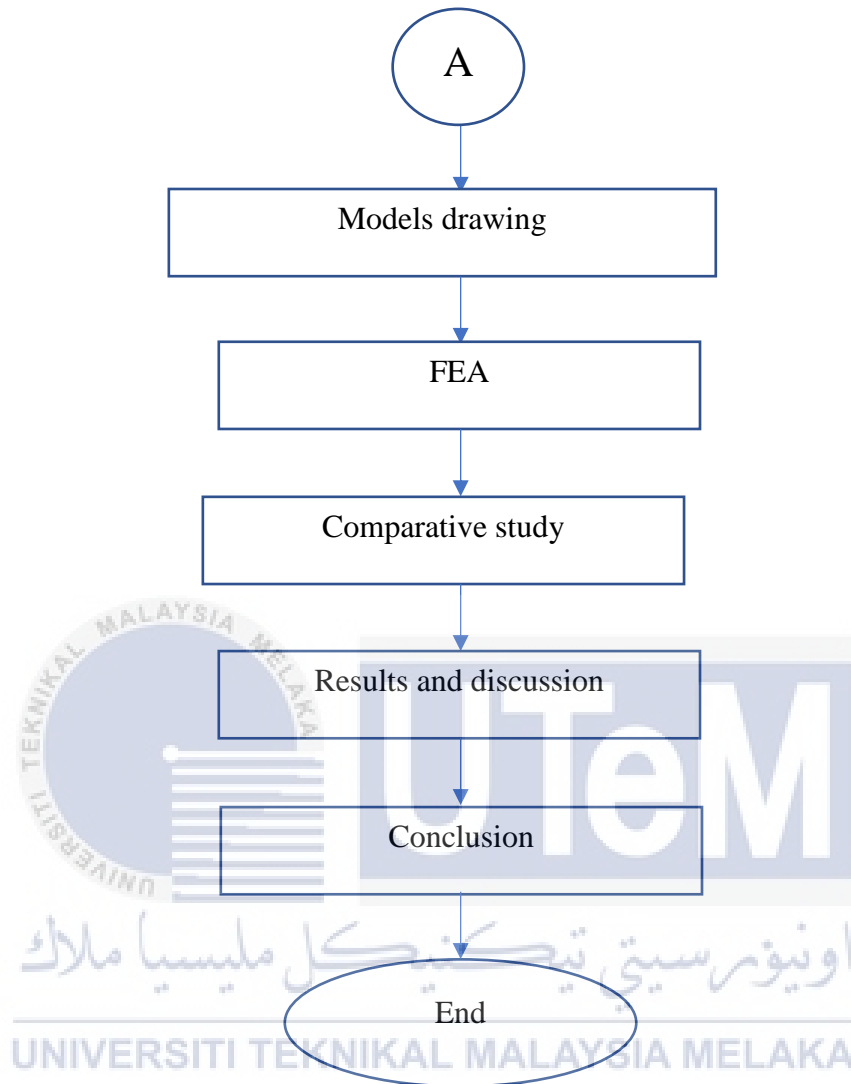


Figure 3. 1 : Overall flow of the experiment.

Table 3. 1 : Gantt chart for PSM 1

Task	W1	W2	W3	W4	W5	W6	W7	W8	W9	W10	W11	W12	W13	W14
Discussion with the supervisor														
Determination of the topic and objectives of the project.														
Literature review														
Report chapter 1														
Preparation on progress report														
Report chapter 2														
Selection of material and specimen preparation														
Report chapter 3														
Submission of draft final report														
PSM 1 seminar														

Table 3. 2 : Gantt chart for PSM 2

Week	1	2	3	4	5	6	7	8	9	10	11	12	13	14	15	16	17	18
<b>Models drawing using SolidWorks</b>	■	■	■															
<b>FEA</b>				■	■	■												
<b>Data analysis</b>						■	■											
<b>Comparative study</b>							■	■	■	■								
<b>Preparation on progress report</b>										■	■	■	■					
<b>Results and discussion</b>												■	■	■	■			
<b>Final report writing</b>											■	■	■	■	■	■	■	
<b>Final report submission</b>																	■	
<b>PSM II seminar</b>																		■

This project starts with the determination of the topic and objectives of the project. The suitable title and objectives of this study were discussed with supervisor based on reading from previous journal and article. The main purpose of this study is to characterize the slit parameters of ferromagnetic material based on magnetic flux leakage by using SolidWorks software. After that, the problems related to this project are identified in order to achieve the targets or objectives of this project. The methodology of this project is then continued by doing the literature review. For this part, all articles that related to the title of the project were downloaded for reading and the necessary information has been highlighted and listed out for literature review in chapter 2. Then, the process of specimen preparation is conducted. Ferromagnetic materials will be used as specimen in this project as the magnetic properties of the material that can easily magnetized when magnetic field is applied. Then, the process is followed by the drawing the model of the specimens by using SolidWorks. The 3D view of the specimen is drawn to ease the analysis proses by using finite element analysis (FEA). After the drawing is completed, the FEA is applied to the model of the specimen to get the distribution of the stress concentration on the specimens. The next step is comparative study. The purpose of the comparative study is to study, analyze and compare the results obtained from the FEA with the existed experimental results from the previous research. The last step is results analysis and discussion. Results analysis is an important stage in any study to determine whether the objectives of the study is achieved or not. The results are then analyzed and evaluated in order to verify the main purpose of the experiment.

### 3.2 SPECIMEN PREPARATION

For this project, the evaluation of ferromagnetic material based on MFL is conducted on nine same size specimen with 5 mm height, 30 mm width and 300 mm length. The length of the specimen is a little bit long in order to minimize the edge effect on the MFL while conducting the experiment. The specimen used in this project is SAE1045 carbon steel. For the process of specimen preparation, the drawing of specimens is designed by using SolidWorks. SolidWorks is a solid modelling software that is commonly used in modelling a design of object or material. Moreover, SolidWorks is convenient to be used in designing the specimens as it allows to design products in 3 dimensions rather than by using CadPac which can only be used to design in 2 dimensions. The designed model of the specimen is as shown in figure 3.2.

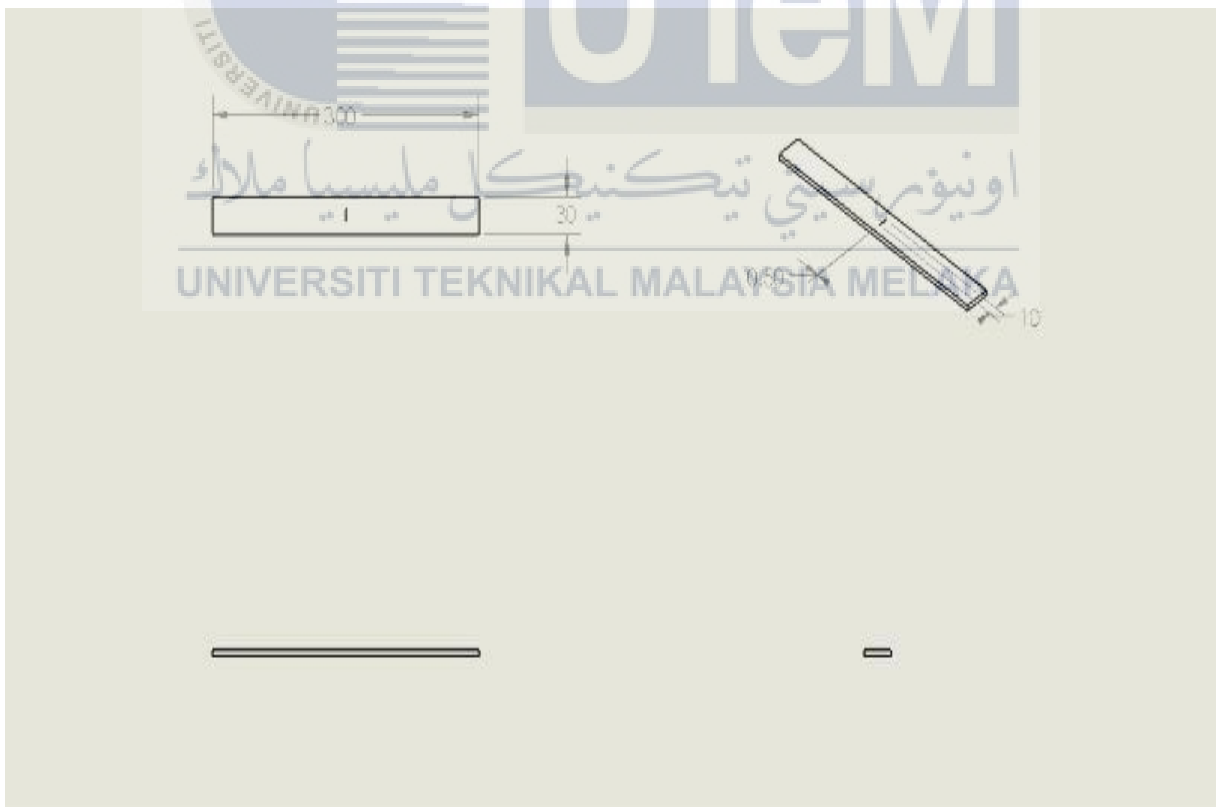


Figure 3. 2 : Design model of specimen.

The different slits or cracks imitation with different parameters is then produced perpendicular to the length of the specimen by using wire cut machine. The slits are produced with different depth and different length as shown in Table 3.2.

Table 3. 3 : Slit parameters of specimen.

Length (mm)	Depth (mm)
3 mm	0.5 mm
	1.0 mm
	1.5 mm
5 mm	0.5 mm
	1.0 mm
	1.5 mm
10 mm	0.5 mm
	1.0 mm
	1.5 mm

### 3.2.1 MATERIAL SELECTION

SAE1045 carbon steel is used as the specimen of this project due to its good weldability and machinability. In addition, SAE1045 carbon steel is a durable material with low maintenance and offers the least cost in comparison with other materials. SAE1045 carbon steel is selected as the specimen of this project due to its advantages. This material is widely used in various structures and machine elements such as shafts, hydraulic tubes, pins, crankshaft and rotors because these materials provide a variety of high strength and ability to meet the needs of the industry (Ibrahim et. al, 2015). Other than that, SAE1045 carbon steel is a good weldability and machinability material as well as low maintenance and offers the least expensive choice in comparison with other materials. In addition, the probability of this material failing such as fatigue is high due to mechanical or structural components undergoing continuous loading. These materials usually experience failures while in service such as material cracks due to the effect of the manufacturing or heat treatment process.

The selection of this material is based on the breakdown of the chemical composition as listed in Table 3.3. SAE1045 carbon steel contains a high content of paramagnetic substances namely Manganese. The outer magnetic field attract the paramagnetic material because the paramagnetic has at least one unpaired electron in the material.

Table 3. 4 : Chemical composition of SAE 1045 carbon steel.

Element	Carbon	Silicon	Sulfur	Manganese	Phosphorus	Cromium	Nickel	Molybdenum
Composition	0.47	0.32	0.005	0.71	0.009	0.18	0.04	0.005

### 3.3 FINITE ELEMENT ANALYSIS (FEA)

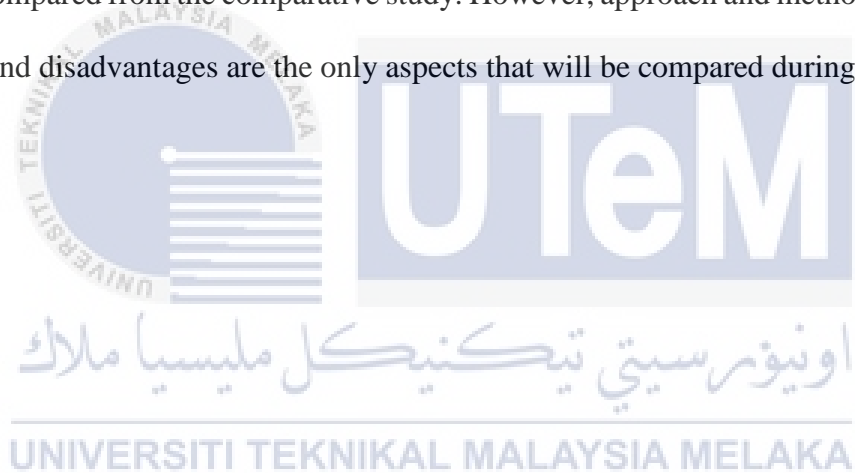
FEA is a computerized method that is used to analyze and predict the reaction of the material to real world forces, heat and other physical effects. For this project, FEA is applied on the model of the specimen in order to get the distribution of stress concentration once 100 N of tension force is applied to the right end side of the model, as shown in Figure 3.3. From the FEA, the results will be tabulated and analyzed to know how the specimens react once force is applied. FEA is one of the important stages during this project for the structural analysis in order to find out the significant stress acting on the materials. It shows either the product will fail or function as it was designed.



Figure 3. 3 : Specimen with 100 N applied force.

### 3.4 Comparative Study

The main purpose of comparative study is to analyze and compare numbers of journal that related to the objectives of this study. For this project, comparative study is made on five journals to compare the stress concentration obtained from the FEA with the experimental results from the previous studies. This comparative study is important to validate whether the obtained distribution of stress concentration is coincident or not with the previous study. By doing so, it will demonstrate how similar or different the results are. There are many approaches that can be compared from the comparative study. However, approach and methodology, results, advantages and disadvantages are the only aspects that will be compared during this project.



## CHAPTER 4

### RESULTS AND DISCUSSIONS

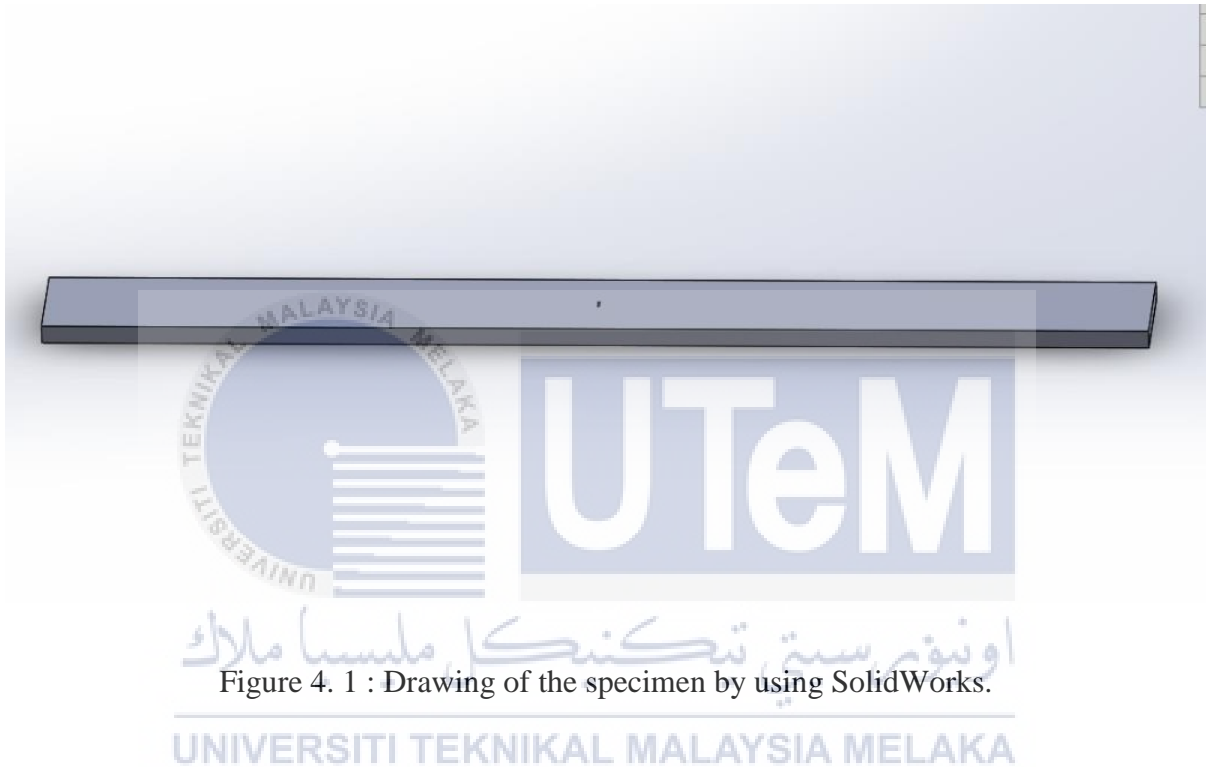
This chapter discusses the results obtained from the FEA which contain Von Misses stress and the distribution of stress concentration on plates with different length and different depth. The data were analyzed and the results for each experiment are tabulated and graphically presented.

This chapter is divided into three sub-section. Section 4.1 explains the FEA conducted on the model of specimen. Then the results obtained from the analysis are tabulated and graphically presented in section 4.2. Lastly, section 4.3 discusses the comparative study which is conducted on five previous experiment from the researches, based on the distribution of stress concentration on the materials.

#### 4.1 RESULTS OF FINITE ELEMENT ANALYSIS (FEA)

FEA is the simulation of physical phenomenon by using a numerical technique known as the Finite Element Method (FEM). It is a computerized method that is used to analyze and predict the reaction of the material once the external load is applied. FEA shows either the product will fail or function as it was designed and will directly help to reduce the physical prototypes produced by running the virtual experiments to optimize the designs. It will help to shorten the time spent to model the different designs and materials instead of spending much time creating multiple iterations of initial prototypes. In addition, FEA is very useful to understand the structural integrity as the structure is made of infinite numbers of atoms. The

process of FEA can be used for the structural analysis to find out the significant stress acting on the materials. It will help to guarantee that the structure is appropriate to provide the utmost performance.



The drawing of the specimen that will be used for this project is as shown in Figure 4.1. FEA or simulation is applied to the 3D drawing of the specimen to analyze how the specimen reacts once force is acting on the specimen. This simulation process starts by selecting the type of materials that is used as specimen, which is SAE1045 steel. After that, the left end side of the specimen is set as fixed geometry and the tension force of 100 N is then applied to the right end of the specimen as shown in Figure 4.2.



Figure 4. 2 : Specimen with fixed geometry and applied force.

Then, the whole specimen body is meshed as shown in Figure 4.3 to subdivide the specimen model into a smaller domains called elements. It is impossible to make the analysis in this format because the continuous object has finite degree of freedom. So, meshing will transform the infinite degrees of freedom to finite, and the domain is break up into pieces which represents each element. In other words, meshing is to actually make the problem solvable using finite element.

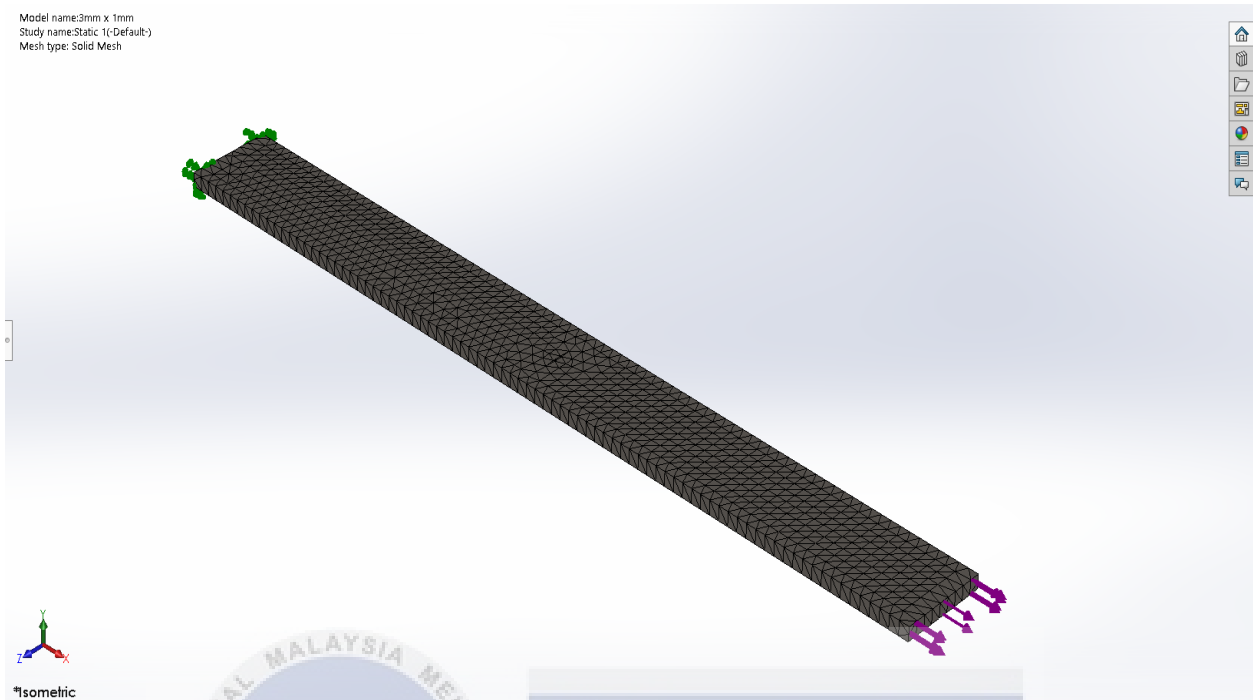
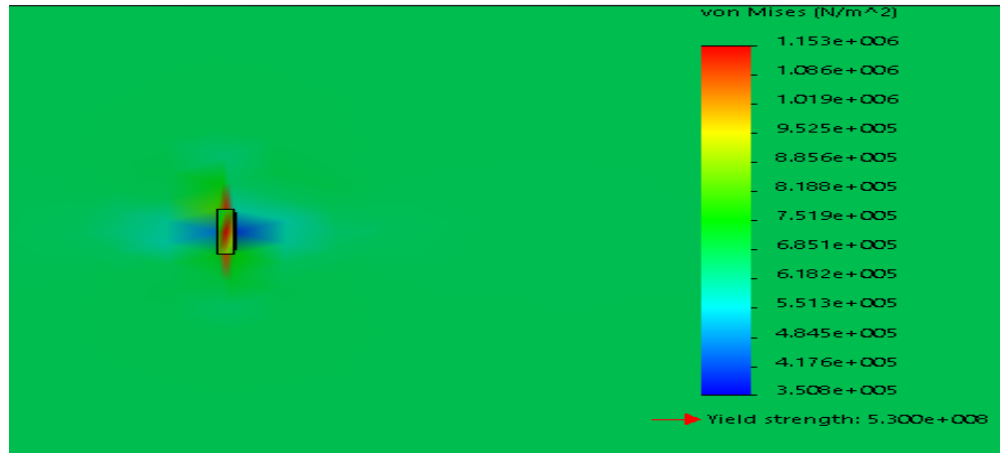


Figure 4. 3 : Meshed specimen model with 50% of mesh density.

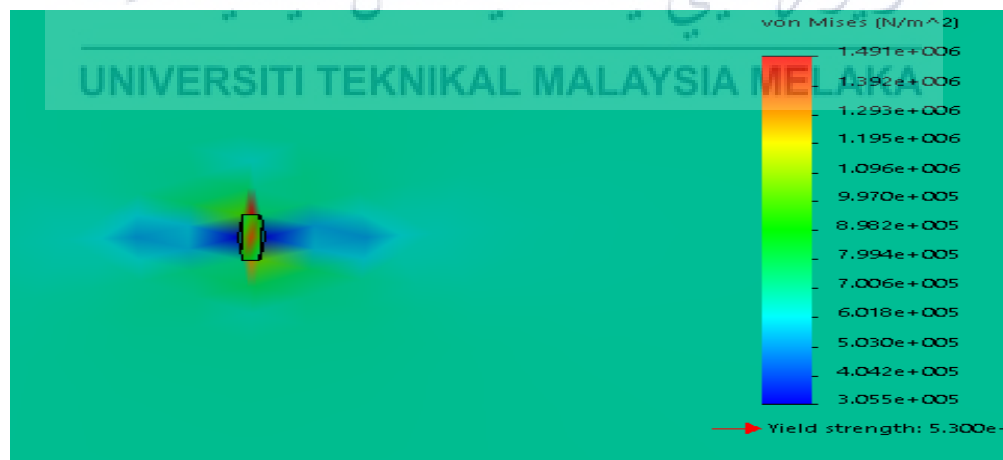
Finally, run the FEA study to produce the distribution of stress concentration as shown in Figure 4.4, Figure 4.5 and Figure 4.6 .



(a)

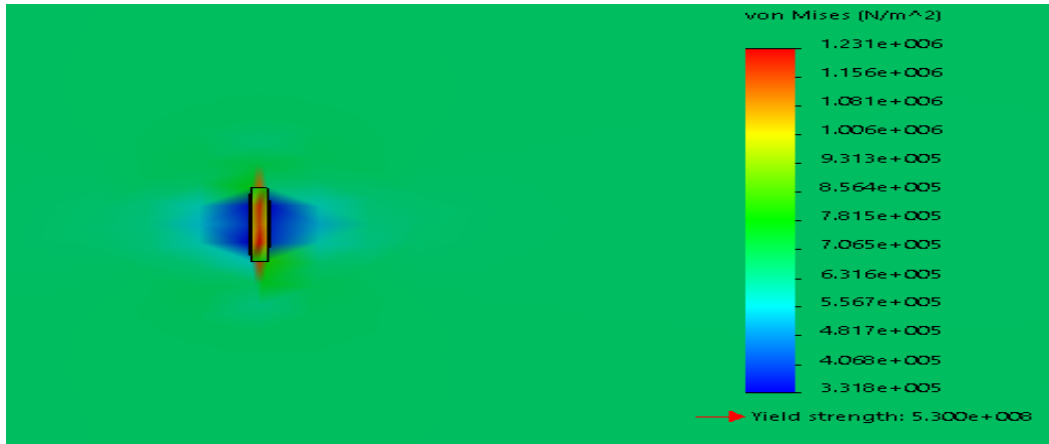


اونيورسيتي تيكنيكل مليسيا ملاك (b)



(c)

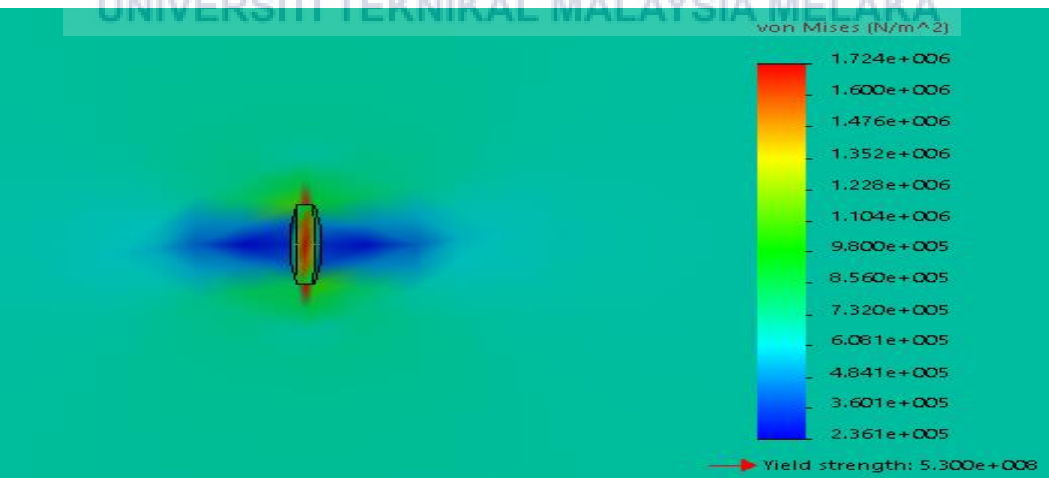
Figure 4. 4 : Von Mises stress distribution of the plate with 3 mm length at different depth (a)0.5 mm (b)1.0 mm (c)1.5 mm



(a)

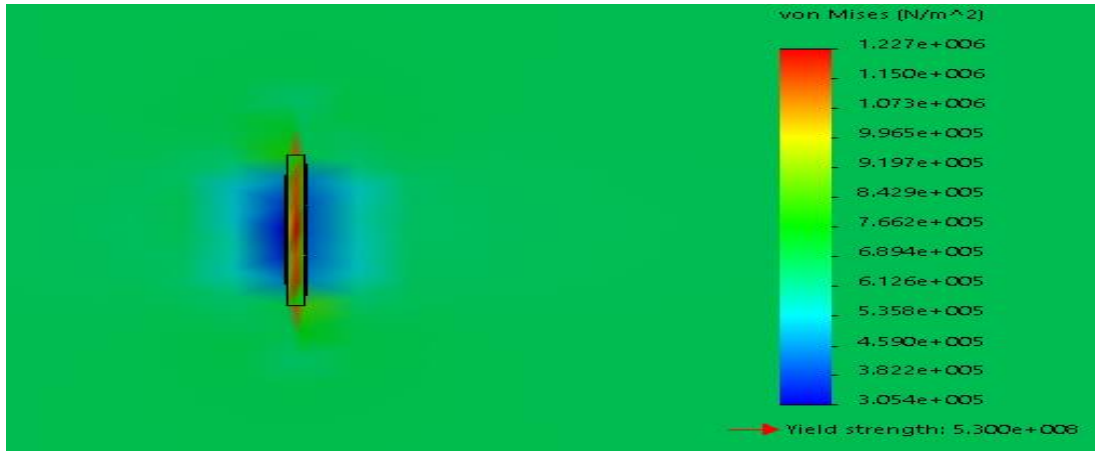


(b)



(c)

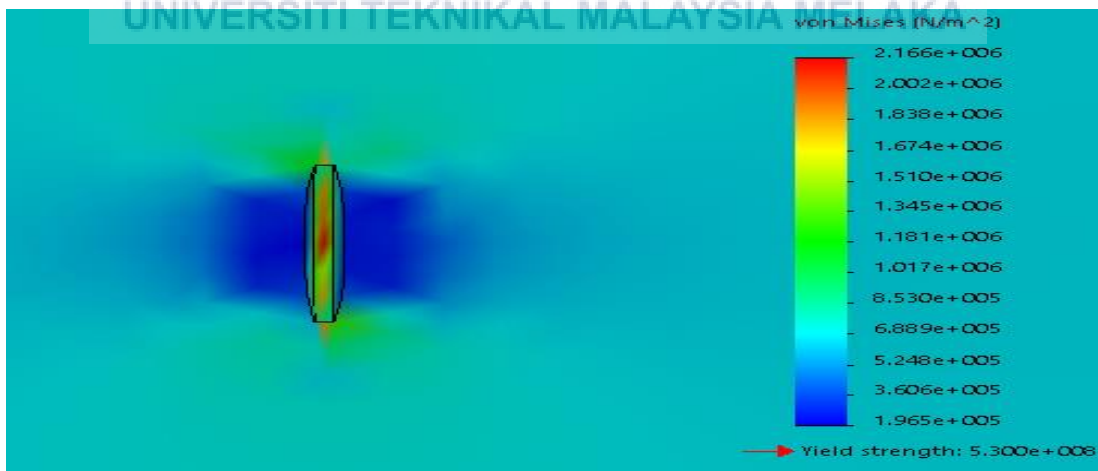
Figure 4. 5 : Von Mises stress distribution of the plate with 5mm length at different depth  
(a)0.5 mm (b)1.0 mm (c)1.5 mm



(a)



(b)



(c)

Figure 4. 6 : Von Mises stress distribution of the plate with 10 mm length at different depth

(a)0.5 mm (b)1.0 mm (c)1.5 mm

## 4.2 GRAPH OF THE DISTRIBUTION OF VON MISSES STRESS.

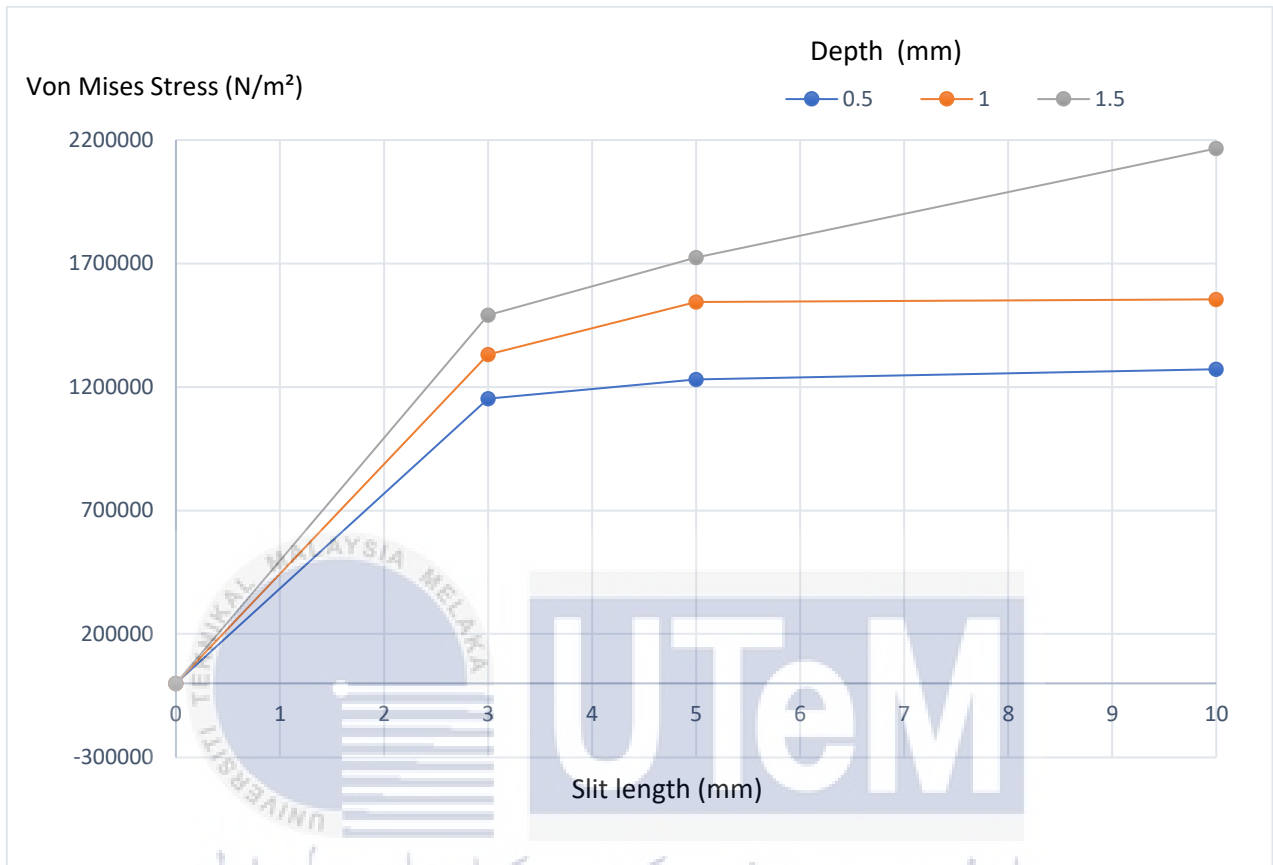


Figure 4. 7.: Graph Von Mises stress vs slit length at 0.5 mm, 1.0 mm and 1.5 mm depth.

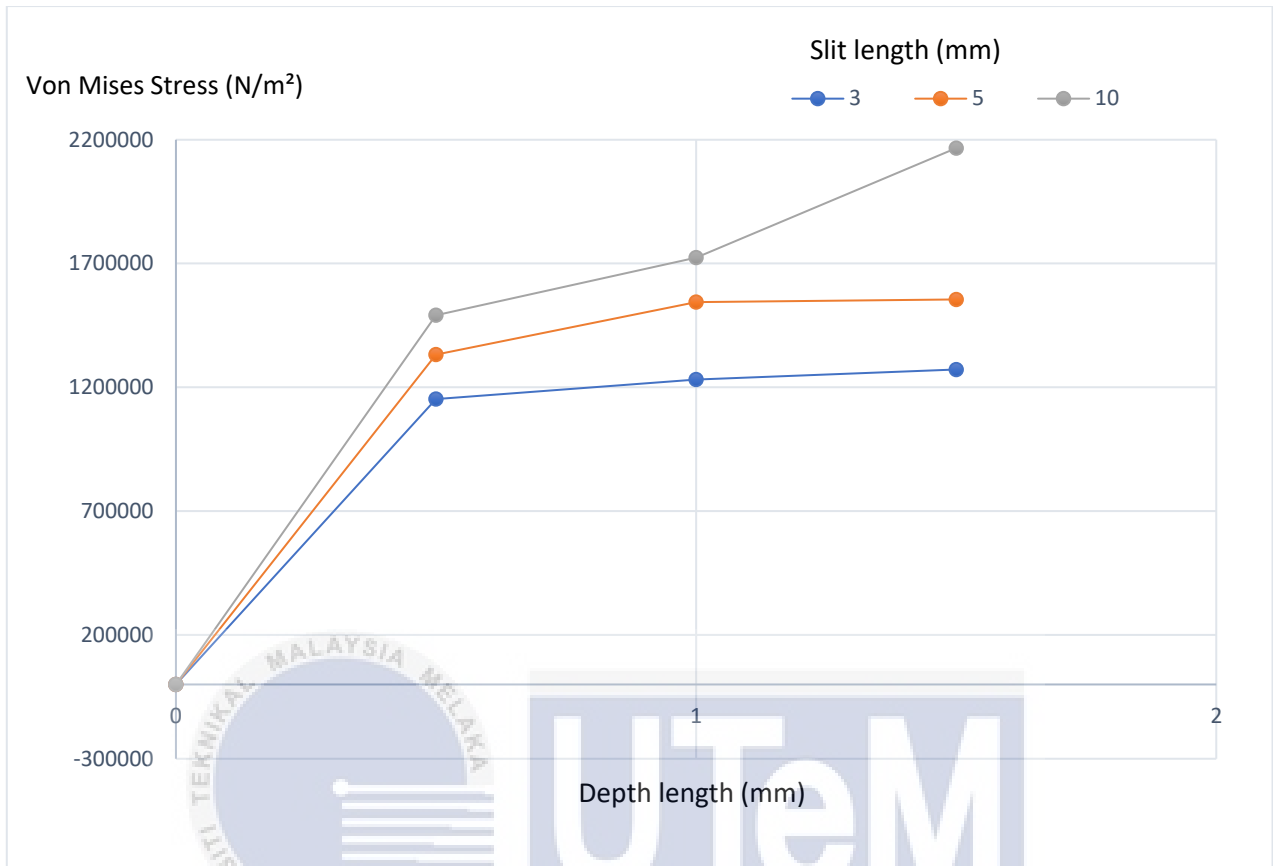


Figure 4. 8 : Graph Von Mises stress vs depth at 3 mm,5 mm and 10 mm slit length.

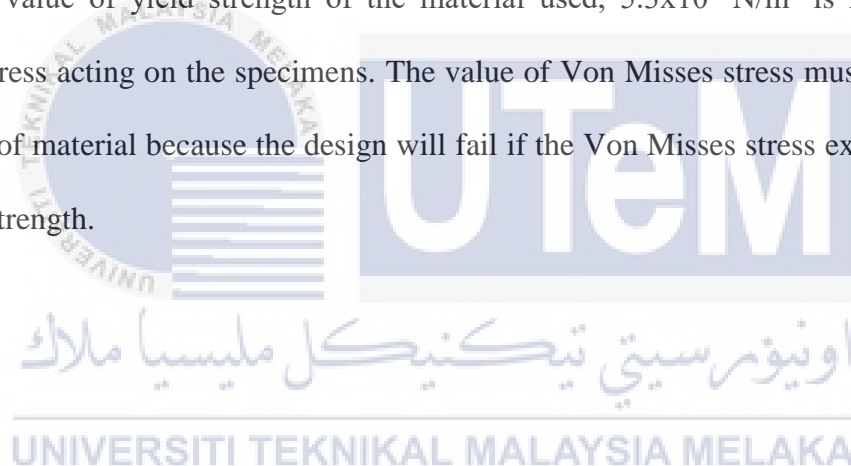
Table 4. 1 : Values of maximum Von Misses stress for different size of slit.

Length (mm)	Depth (mm)	Maximum Von Misses stress (N/m <sup>2</sup> )
3 mm	0.5 mm	1.153 x 10 <sup>6</sup>
	1.0 mm	1.332 x 10 <sup>6</sup>
	1.5 mm	1.491 x 10 <sup>6</sup>
5 mm	0.5 mm	1.231 x 10 <sup>6</sup>
	1.0 mm	1.544 x 10 <sup>6</sup>
	1.5 mm	1.724 x 10 <sup>6</sup>
10 mm	0.5 mm	1.227 x 10 <sup>6</sup>
	1.0 mm	1.555 x 10 <sup>6</sup>
	1.5 mm	2.166x10 <sup>6</sup>

Figure 4.7, Figure 4.8 and Table 4.1 illustrate that the stress distribution varies with different slit length and depth parameters. From the FEA that is conducted on the specimen, it shows that the stress concentration will increase when the slit depth increase. The figures also show that the stress concentration increase when the length of the slit increase. However, it is proven that the depth of the slit gives more influence to the stress concentration than the length of the slit. For examples at the same length (5 mm) but with different depth, the value of the Von Mises stress increase much higher from 1.544x10<sup>6</sup> N/m<sup>2</sup> to 1.724x10<sup>6</sup> N/m<sup>2</sup> at 1 mm and 1.5 mm depth respectively. In contrast, at the same depth (1 mm) with different length of the slit, there are just a small increment in the value of the Von Misses stress which is from 1.544x10<sup>6</sup> N/m<sup>2</sup> to 1.555x10<sup>6</sup> N/m<sup>2</sup> at 5 mm and 10 mm length respectively. In addition, it can

be concluded that the highest value of the Von mises stress is at the largest size of slit which is at 10 mm slit length and 1.5 mm depth with  $2.166 \times 10^6$  N/m<sup>2</sup> while the smallest value is at the smallest size of slit with  $1.153 \times 10^6$  N/m<sup>2</sup>.

Von Mises stress is a metric of measurement used to determine whether the material will yield or fracture at any point. The stresses that are calculated at any point can be mathematically written into a scalar quantity known as Von Mises stress, which then can be compared with experimentally observed yield points. By using this information, the failure of the design can be predicted. From the results of the analysis, we can predict that the specimens are safe to be used because the value of yield strength of the material used,  $5.3 \times 10^8$  N/m<sup>2</sup> is higher than the maximum stress acting on the specimens. The value of Von Misses stress must be lower than the strength of material because the design will fail if the Von Misses stress exceeds the value of material strength.



### 4.3 COMPARATIVE STUDY

Comparative study is a study to compare and analyze two or more ideas involving understanding, observing and explaining all aspects or events. It can help to demonstrate ability to analyze, compare and contrast topics or ideas. By doing so, it will demonstrate how similar or different the concepts are. The aim of this comparative study is to compare the results of stress concentration obtained from the FEA with recent studies. The comparison is made between five experiments recently conducted by numerous researchers in the aspect of approach and methodology, results, advantages and disadvantages.

#### 4.3.1 FIRST EXPERIMENT

For the first experiment conducted by Wang et. al, (2010), it is aimed to present some quantitative study about the characteristic of the defects effected on self-magnetic flux leakage(SMFL) signals in the stress concentration zone. MMM technique has recently attracted great interest in NDT due to its special advantages. However, the mechanism of MMM is not clearly classified as the MMM technique can detect the position of defect, without describing the characteristics of the defect. In order to promote study in this area, a linear magnetic-charge model is used to evaluate the distribution of SMFL in the local stress concentration. This model helps to produce the data on SMFL signals from the effects of defects depth and location.

Ferromagnetic SMFL signal is generated along the stress concentration zone. From the experimental observations, the tangential SMFL component,  $H_{P(x)}$  exhibits maximum while the normal component  $H_{P(y)}$  exhibits zero in the maximum stress concentration zone, as shown in Figure 4.9.

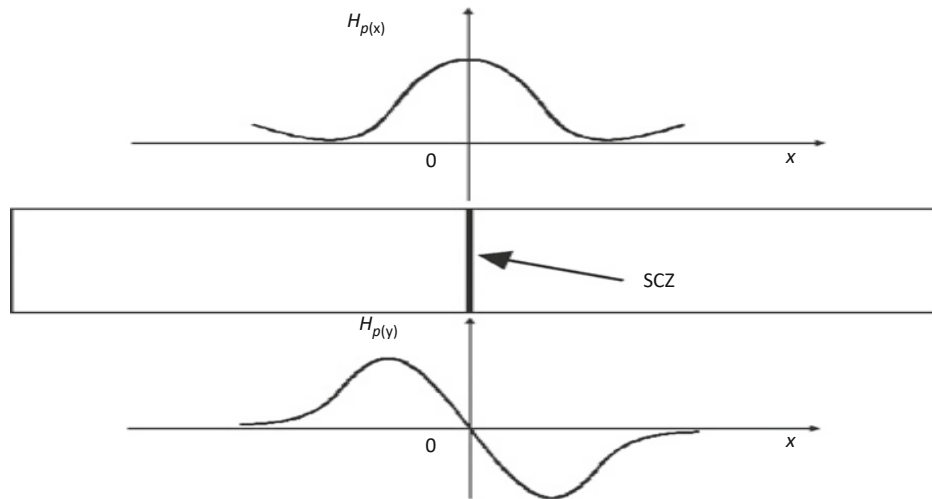


Figure 4. 9 : Schematic view of SMFL distribution in the stress concentration zone.

A rectangular defect imitation with  $b$  and  $d$  represent width and depth respectively, is considered in this experiment. Figure 4.10 represent the  $H_{p(x)}$  and  $H_{p(y)}$  along the stress concentration zone, which achieved from  $d=2$  mm,  $b=3$  mm and lift-off value of  $Y=0.5$  mm. In the maximum stress concentration zone, the theoretical results are similar to the experimental observation where  $H_{p(x)}$  reaches a peak and  $H_{p(y)}$  changes its polarity.

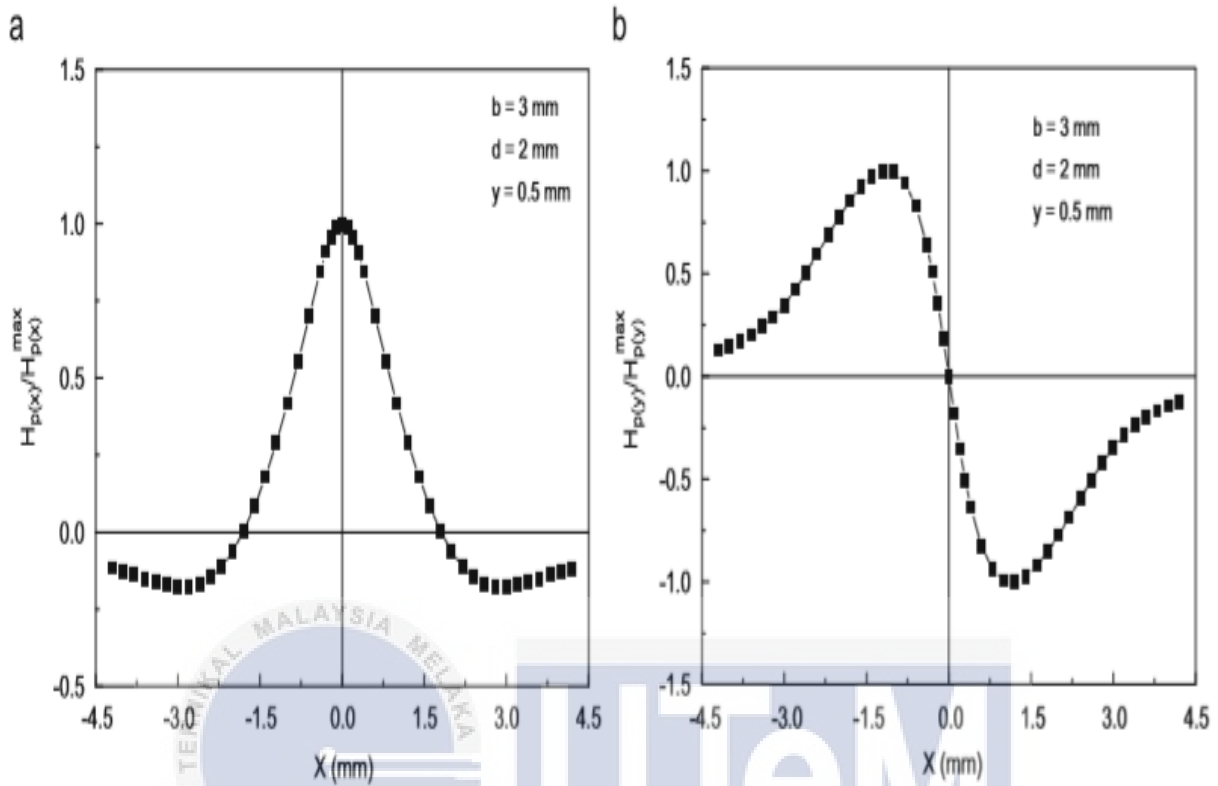


Figure 4. 10 : Distribution of normalized tangential and normal component along the x-axis direction.

In this study, the defect location and defect depth are specially considered. The distributions of normalized SMFL components are shown in Figure 4.11. From the distribution of SMFL, when the depth of defect increase from 1 mm to 2 mm, the normal and tangential SMFL amplitudes also increase. However, when the defect depth increase from 2 mm to 3 mm, there are significant different on the SMFL components. For more clear understanding, peak amplitudes of SMFL signals with defect depths from 0.2 mm to 3.0 mm are shown in Figure 4.12. The values are listed in Table 4.2.

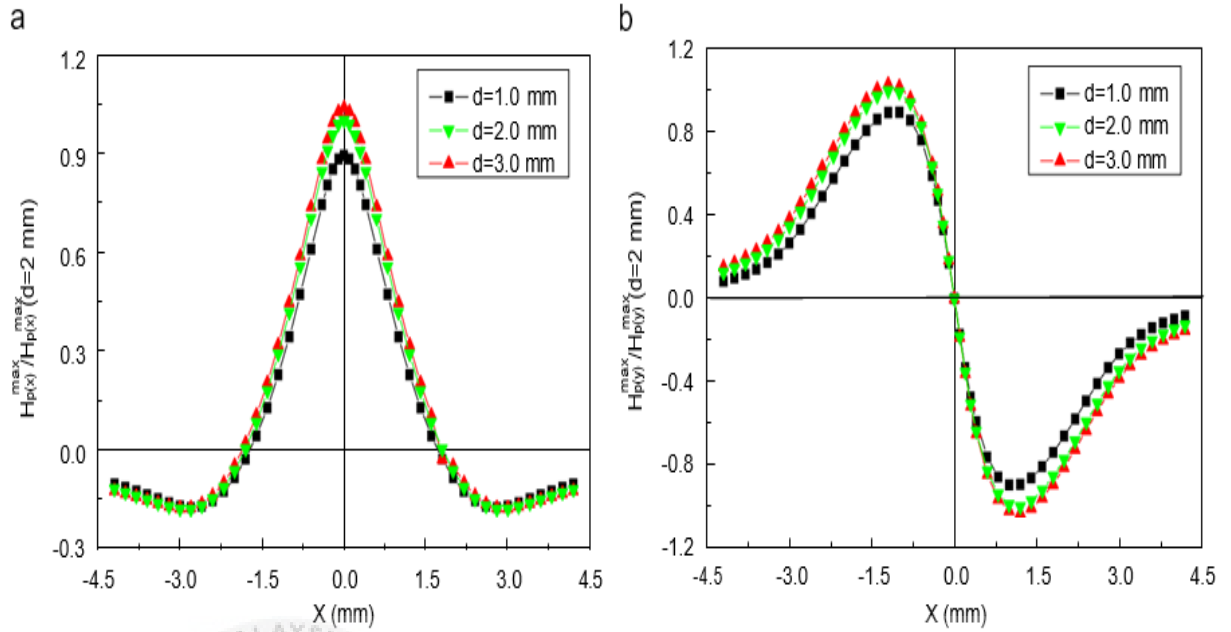


Figure 4. 11 : SMFL signal versus defect depth : (a) tangential component and (b) normal component.

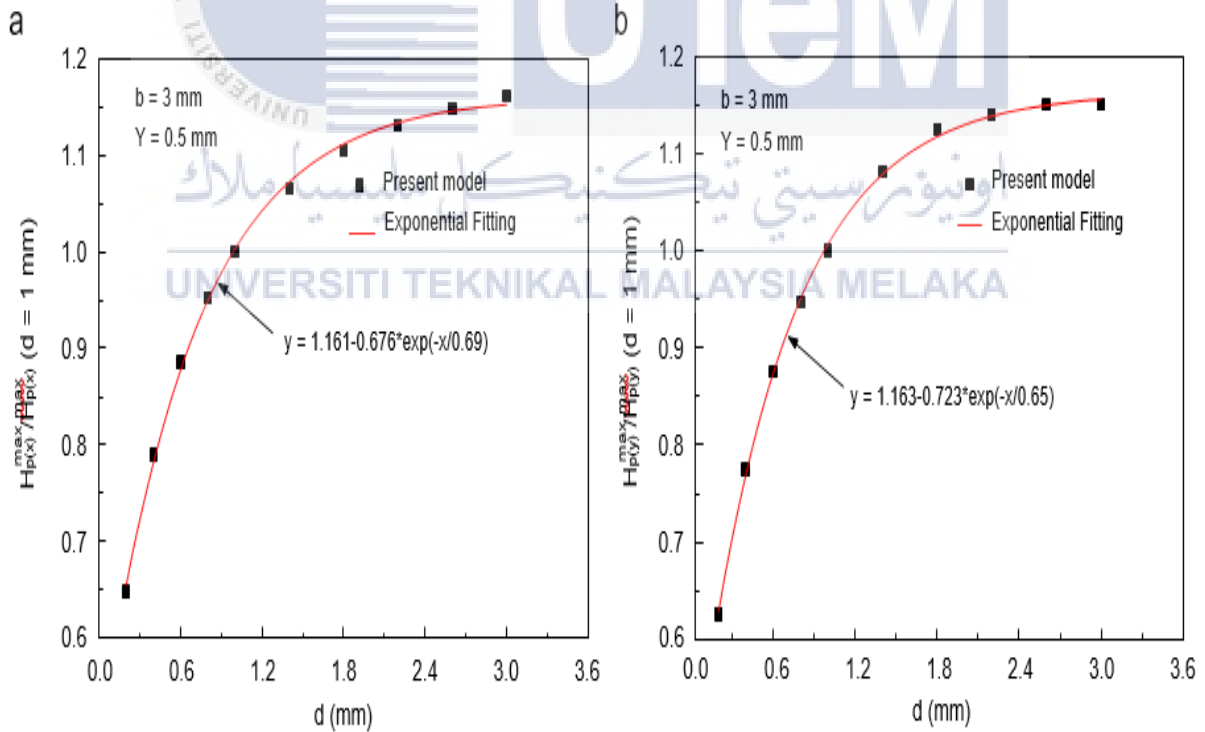


Figure 4. 12 : Influence of defect depth on the normalized SMFL amplitudes :

(a) tangential component and (b) normal component.

Table 4. 2 : Values of defect depth.

Defect depth (mm)	Normalized values in $x$ -axis	Normalized values in $y$ -axis
0.2	0.6483	0.62627
0.4	0.79034	0.77539
0.6	0.88503	0.876
0.8	0.95147	0.94637
1.0	1	1
1.4	1.06453	1.08086
1.8	1.10424	1.12451
2.2	1.13032	1.13979
2.6	1.14828	1.15008
3.0	1.16114	1.15008

From Figure 4.12, it illustrates that the surface defect gives more influence on the SMFL signals compared to the inner defects. In engineering structures, the inner defects are more complicated to be analyzed compared to the surface defects. Figure 4.13 shows the SMFL distributions, where  $w$  is the distance of the defect from the specimen surface. The results shows that both  $H_{p(x)}$  and  $H_{p(y)}$  decrease when  $w$  increase, while there is no change in SMFL range. For a better understanding, the values of  $w$  from 0 mm to 1.5 mm are studied. Figure 4.14 presents the results while the detailed data is listed in Table 4.3.

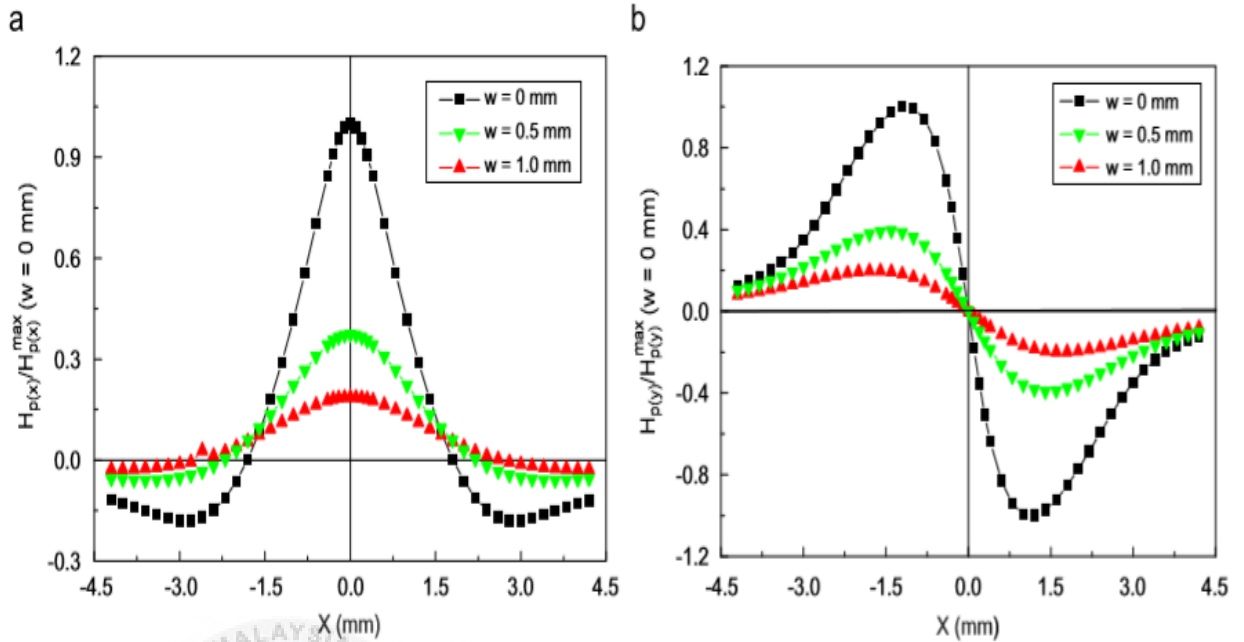


Figure 4. 13 : SMFL signal versus  $w$  ( $Y=0.5$  mm,  $b=3$  mm,  $d=2$  mm) : (a)tangential component and (b) normal component.

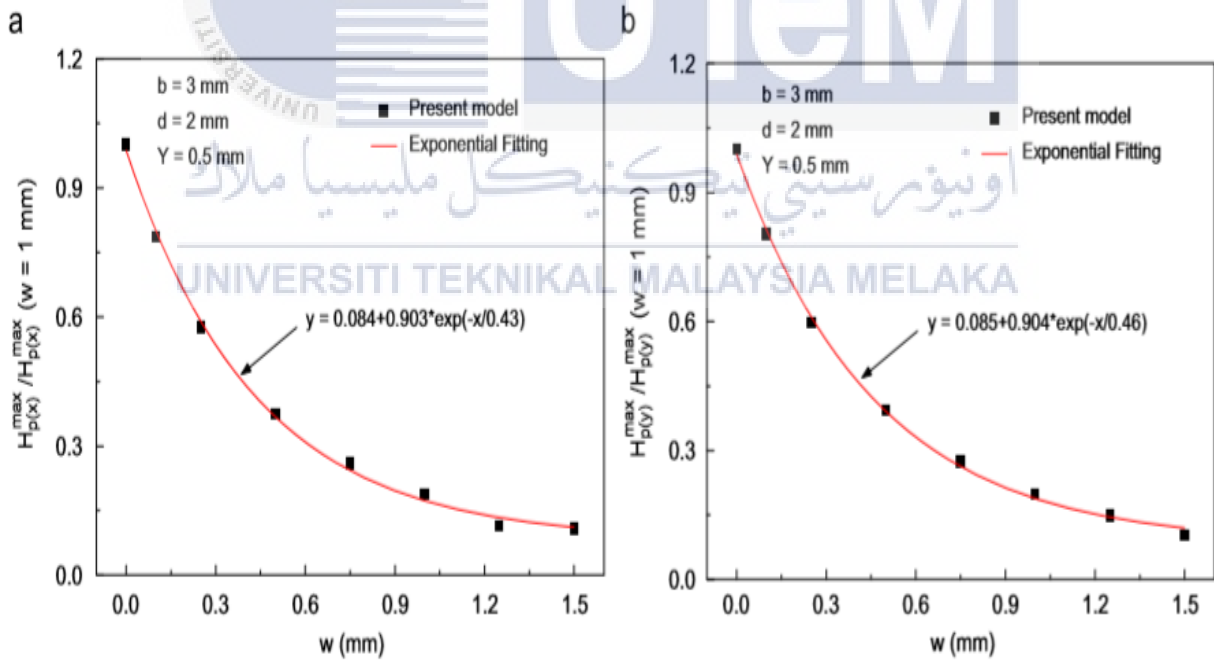


Figure 4. 14 : Influence of  $w$  on the normalized SMFL amplitudes :  
(a) tangential component and (b) normal component.

Table 4. 3 : values of defect location.

Defect location (mm)	Normalized values in $x$ -axis	Normalized values in $y$ -axis
0	1	1
0.1	0.787017	0.802857
0.25	0.576516	0.598601
0.5	0.37313	0.392966
0.75	0.258446	0.27374
1	0.187441	0.198176
1.25	0.114464	0.148832
1.5	0.108443	0.103505

From figure 4.14, it shows that the normalized SMFL amplitudes decrease when  $w$  increases from 0 mm to 1.5 mm, respectively. This means that the amplitude decrease when the distance of the defect from the surface increase. However, there is no significant difference resulted between normalized  $x$ -axis and  $y$ -axis components. From figure 4.14, the fitting results and theoretical value are much agreeable.

### 4.3.2 SECOND EXPERIMENT

In this paper Zhong et.al, (2010) investigate the relation of magnetic signals of stress concentration and the magnetic environment. The theory-based NDT methods such as the MMM method has been proved to be used to measure the stress concentration on the specimens. However, the magneto-mechanical effect model theory produced is based on the linear stress distribution and the effect of environmental magnetic field on the stress concentration is still unclear. From previous study, the testing result was inaccurate because the effect of the magnetic environment is not considered. Figure 4.15 shows the experimental system used to monitor the stress status and the field of magnetic environment during detection.



Figure 4. 15 : Experimental system :

(A)3D Helmholtz coil, (B)Portable tensile means, (C)Specimens, (D)Flux gate magnetometer and Tesla magnetometer, (E)3D displacement controller, (F)Wireless micro-magnetic detector, (G)Computer.

3D magnetic Helmholtz coil system is to produce a constant magnetic field from 220 to 20 Gs to maintain the environmental magnetic field. To ensure the effectiveness of 3D magnetic Helmholtz coil, the Tesla magnetometer and flux gate magnetometer are used in this experiment. Tension force controller, which made of aluminium, is used in order to provide tension force from 0 N to 200 N. The computer contains a 3D displacement controller and a wireless micro-magnetic detector is used to monitor the magnetic field which is perpendicular to the surface of the specimen, as shown in Figure 4.16.

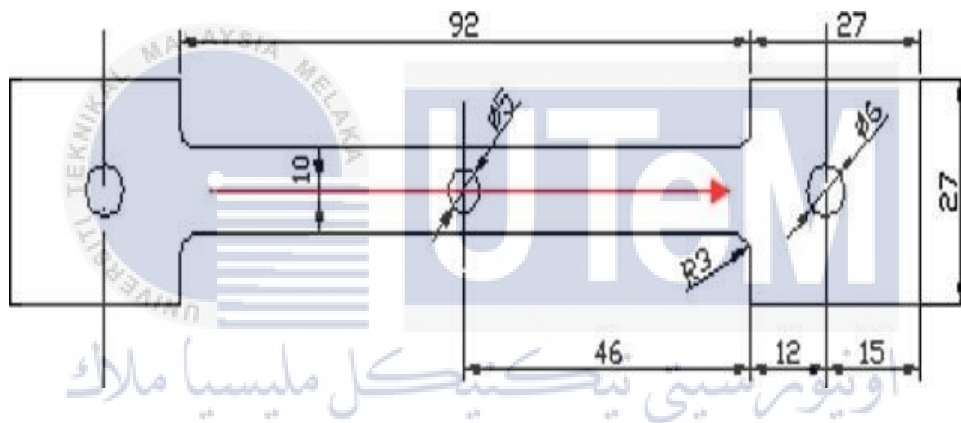


Figure 4. 16 : Specimen dimension and scanning line.

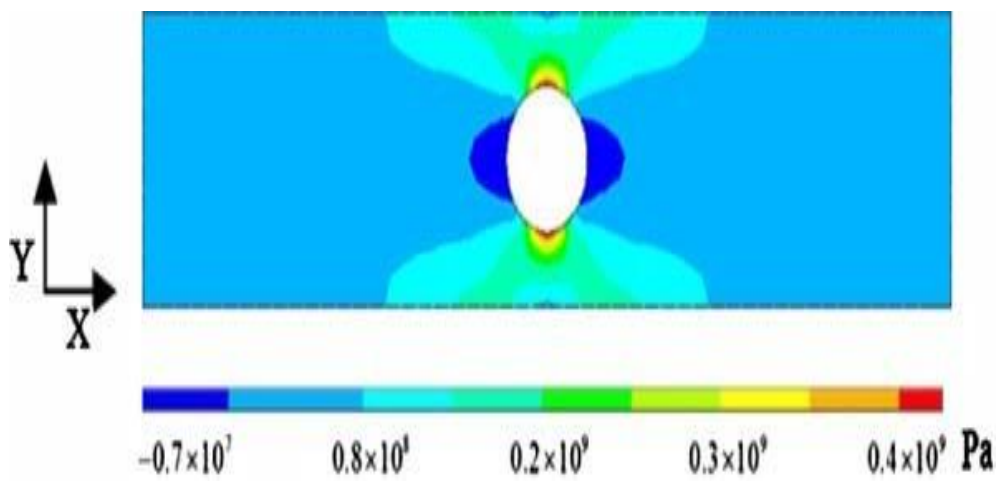


Figure 4. 17 : The distribution of stress on the scanning line

For this experiment, 45C carbon steel is used as the specimens. Physical properties and chemical components of the materials are as listed in Table 4.4 and Table 4.5 while Figure 4.16 illustrates the specimen. The stress concentration will distribute around the hole once the specimen is subjected to tensile force, as shown in Figure 4.17 by using FEA.

Table 4. 4 : Physical properties of the material.

$\sigma_b$ (MPa)	$\sigma_s$ (MPa)	$\delta_5$ (%)
608	353	17

Table 4. 5 : Components of the material.

C (wt%)	Si (wt%)	Mn (wt%)	P	S	Cr	Ni	Cu
0.36–0.45	0.14–0.40	0.47–0.83	<0.040	<0.040	<0.28	<0.28	<0.28

Figure 4.18 shows that the magnetic field on the end of the scanning line in environmental magnetic field of 14 Gs is out of the sensor's testing range (6 Gs). The abnormality of the magnetic field is detected near the stress concentration around the hole. From the results obtained, the slope caused by the entire magnetization, defect by stress concentration and defect by hole in the centre influence the magnetic distribution. From the results, the defect by hole is the abnormality of the field since the tension force does not cause obvious plastic deformation. The data at the middle scanning line is considered for analysis in order to minimize the edge effect.

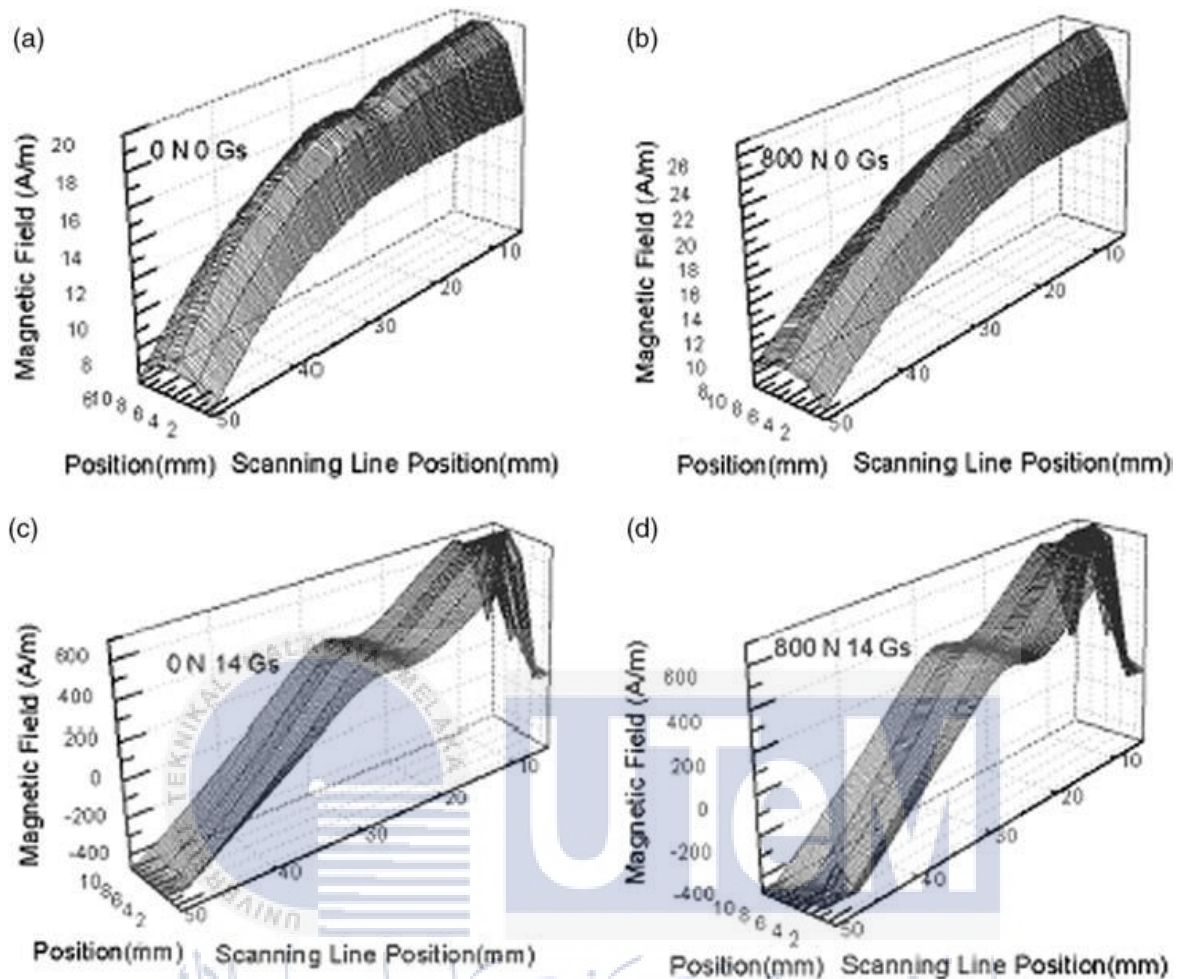


Figure 4. 18 : Magnetic distribution perpendicular to the surface of specimens.

UNIVERSITI TEKNIKAL MALAYSIA MELAKA

The result after data processing is shown in Figure 4.19, which is considered as the defect caused by stress concentration. Although stress concentration is still the same, the results varies in different magnetic field due to the environmental magnetic field. Sometimes, the magnetic environment gives more influence than the stress concentration. From Figure 4.19, it shows that the changing tendency when the environmental magnetic field higher than 14 Gs is differs with the tendency of environmental field lower than 12 Gs. This is because during the tension loading process, it was assumed that there is no plastic deformation. However, in reality, it exists during the detection.

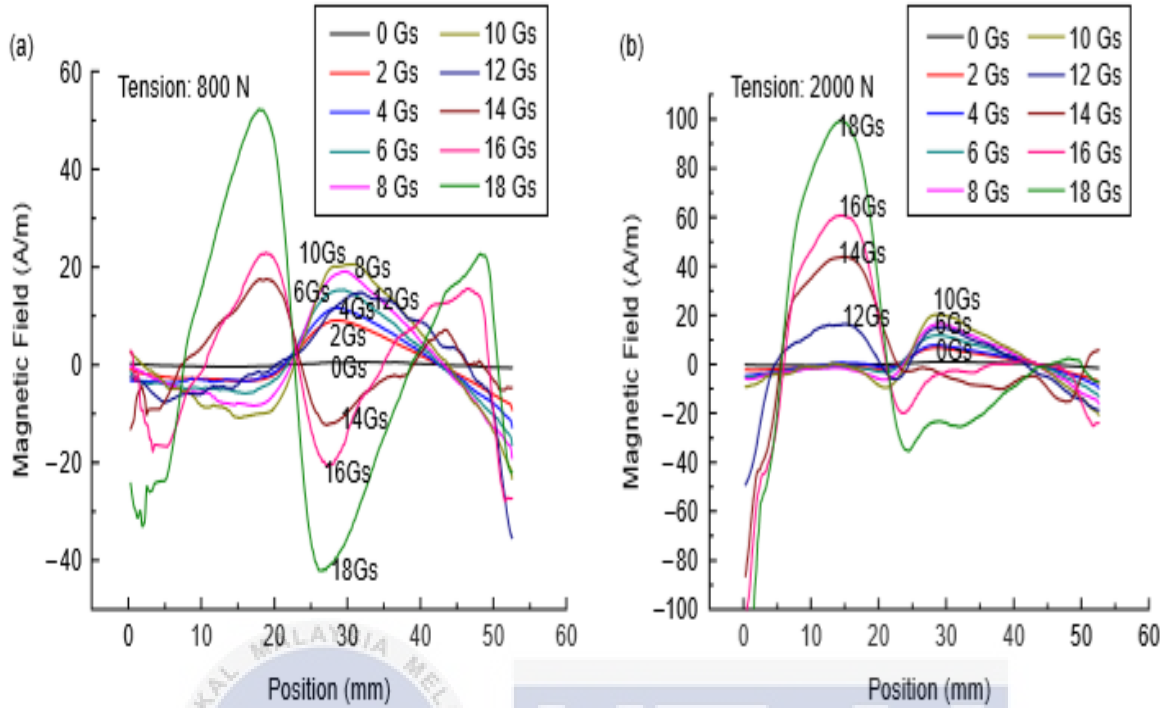


Figure 4. 19 : Magnetic abnormality caused by different level of stress concentration on the scanning line : (a) with a tension of 800 N, (b) with a tension of 2000 N.

Testing the surface magnetic field in different environmental magnetic fields can help to evaluate the stress concentration because the result of stress concentration just by considering the amplitude of magnetic defect is inaccurate. To obtain a quantifying result of stress concentration in industrial applications through the weak-magnetism inspection technology, a mathematical model is needed, which might be complicated because it involves several factors such as material status and magnetic environment. However, most research on the magneto-mechanical effect theory is based on the precondition that the stress distribution is linear in a very small area. Therefore, a lot of work are still needed to obtain the mechanical model for a nonlinear stress concentration.

### 4.3.3 THIRD EXPERIMENT

For the third experiment conducted by Xin'en et al, (2019), it is aimed to propose a method to identify geometrical defects and stress concentration zones in MMM method. In ferromagnetic components, there may be both stress concentration zones and geometric defects. The existence of both defects often leads to the evaluation of MMM technique becomes complicated.

There are several types of numerical simulation method that can be used to distinguish the two types of defect, for examples are boundary element method and FEM. In this paper, a method of analyzing the 3D magneto-mechanical coupling of finite elements is study to produce the MFL signals of an X80 pipeline steel plate. The X80 pipeline steel plate with a centre hole is study and the effects of the hole and the stress-concentration zones was analyzed, then the two types of damage is identified.

For many years, MMM method is used in the inspection of oil and gas pipelines. The circumferential tension stress  $\sigma_{\theta}$  is the maximum stress component for an in-service pipeline because internal pressure  $q$  is the main load for it, as shown in Figure 4.20. The pipeline as shown in Figure 4.21 is therefore being studied, instead of pipelines subjected to internal pressure with corresponding damage. The multi physics analysis software ANSYS is used to study the MFL finite element simulation in which the magnetic anisotropy constitutive model 3D stress-induced above was integrated.

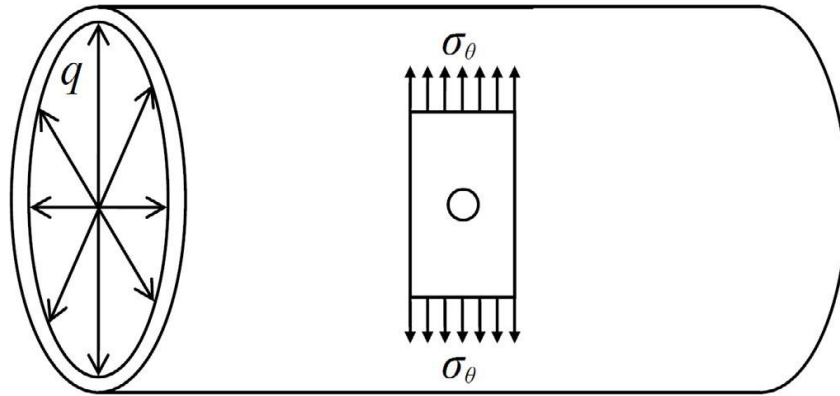


Figure 4. 20 : Pipelines subjected to internal pressure.

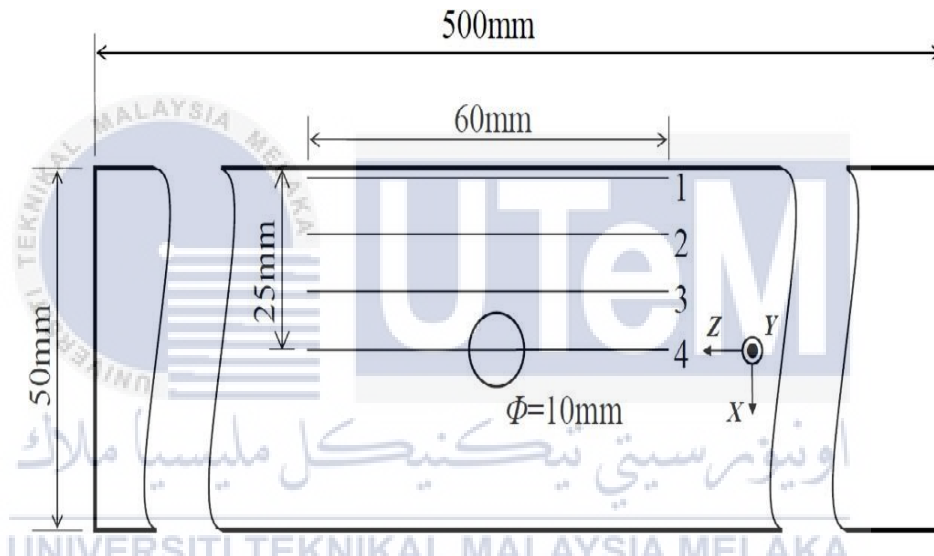
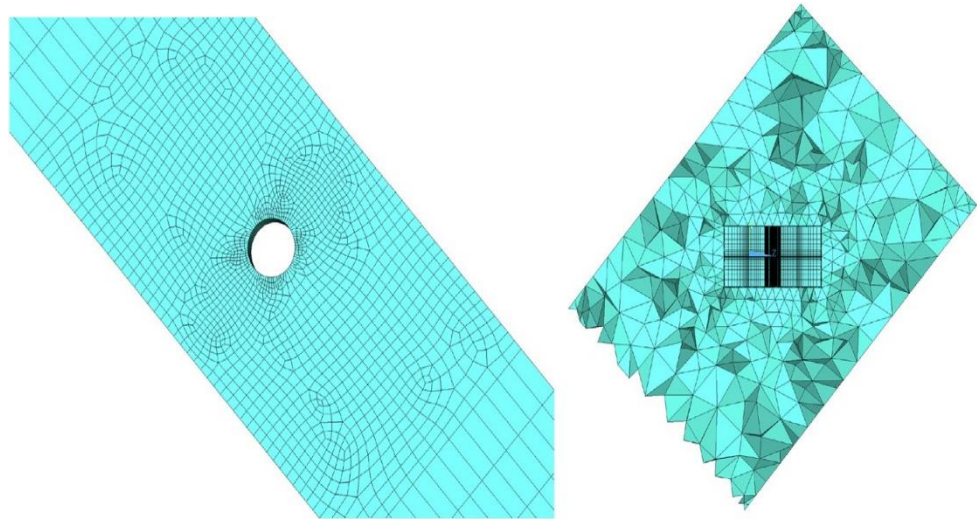


Figure 4. 21 : Schematic of specimen with the thickness of 5 mm.

Figure 4.22 shows the finite element models of the specimen and the surrounding air region. Although it is proved that measuring the locations depends on the geomagnetic field, it can be considered approximately as a uniform field in a relatively small space. The measured data is used to determine the magnitude and direction of the geomagnetic field used in the simulation.



(a) The plate model with a hole

(b) The air model (the inner is the specimen)

Figure 4. 22 : Finite elements model of the specimen and the surrounding air region.

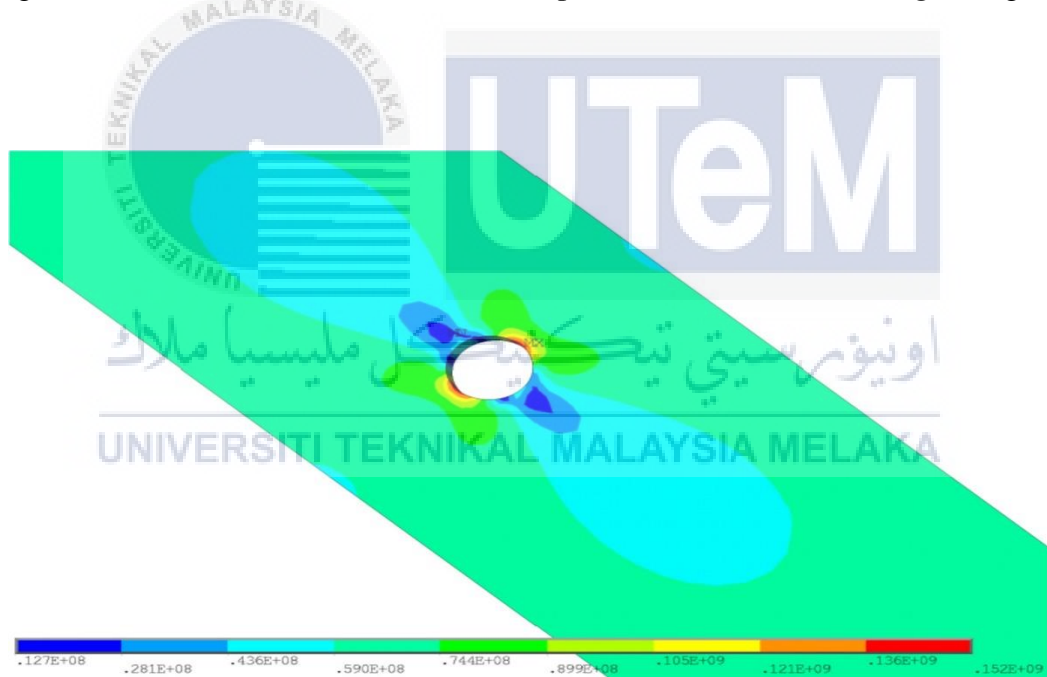
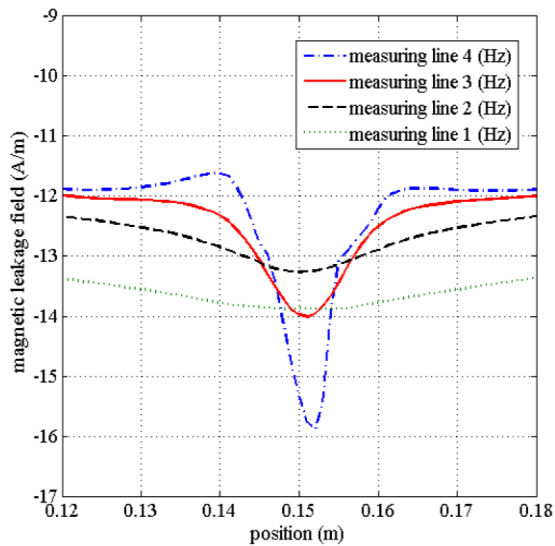
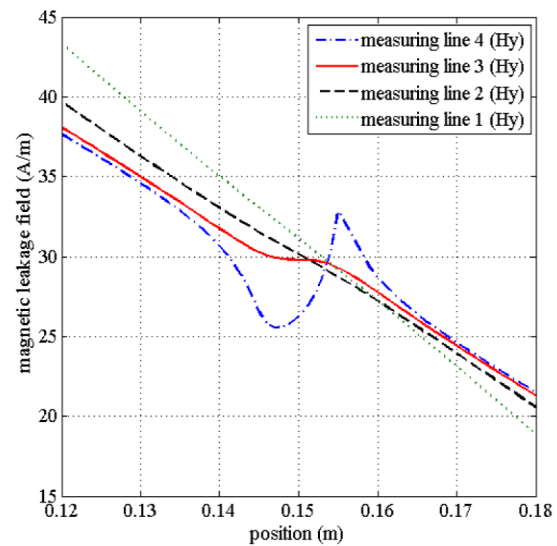


Figure 4. 23 : Von Mises equivalent stress for the specimen under tensile load (12.7 kN).

Figure 4.23 shows the Von Mises stress obtained from the simulation of the specimen with a load of 12.7 kN. The results represent that there are two local stress-concentration zones around the hole. Figure 4.24 shows the characteristics of the MFL signals induced by geometry defects and stress concentration.



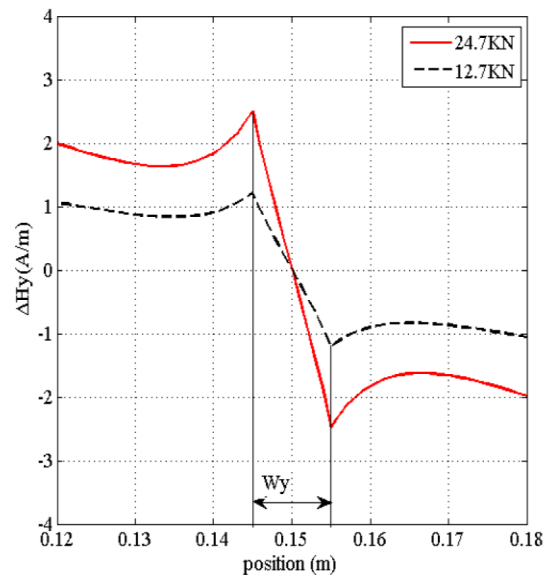
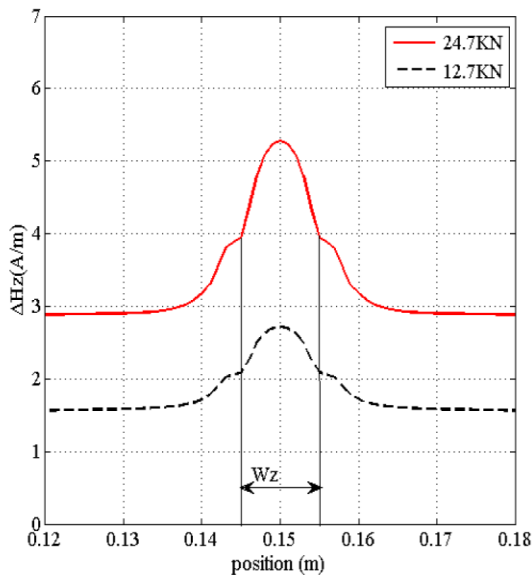
(a) The tangential component of the MFL



(b) The normal component of the MFL

Figure 4. 24 : The MFL simulation results along different measuring lines under tensile load (12.7 kN)

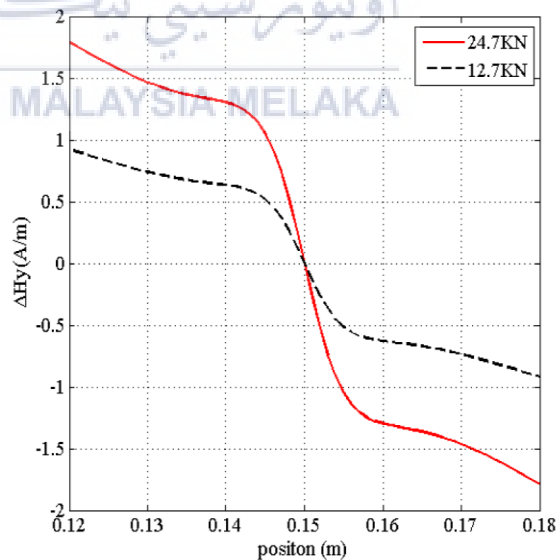
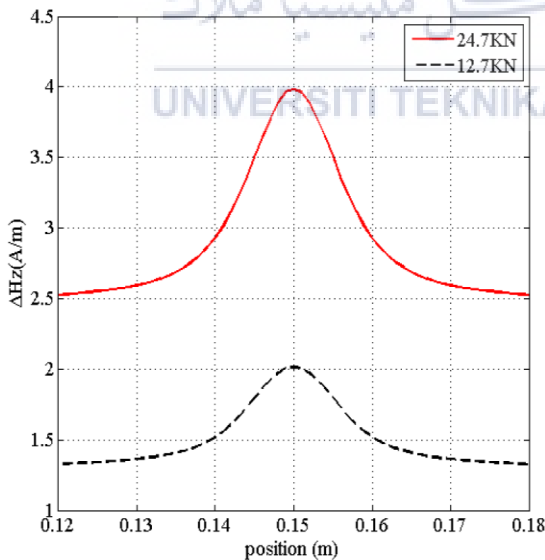
For the measuring line 2 and measuring line 1 in Figure 4.24, the  $H_z$  and  $H_y$  curves have a symmetrical amplitude variation and appear almost linear, respectively. This shows the same results for the specimen without a hole with the MFL curves. It means that there is no effect of the local stress concentration and hole on the MFL signals of line 2 and line 1. However, both MFL signals of line 4 and line 3 are affected by the stress concentration and hole. Therefore, it is clearly complicated to analyze both defects only by the MFL signals due to the similar local characteristics shown by the signals induced by the two types of defects. The MFL differences are calculated by subtracting the reference values with the MFL values under different loads, where the reference values are the MFL curve before loading.



(a) Difference of tangential component for MFL

(b) Difference of normal component for MFL

Figure 4. 25 : MFL differences before and after loading (measuring line 4).



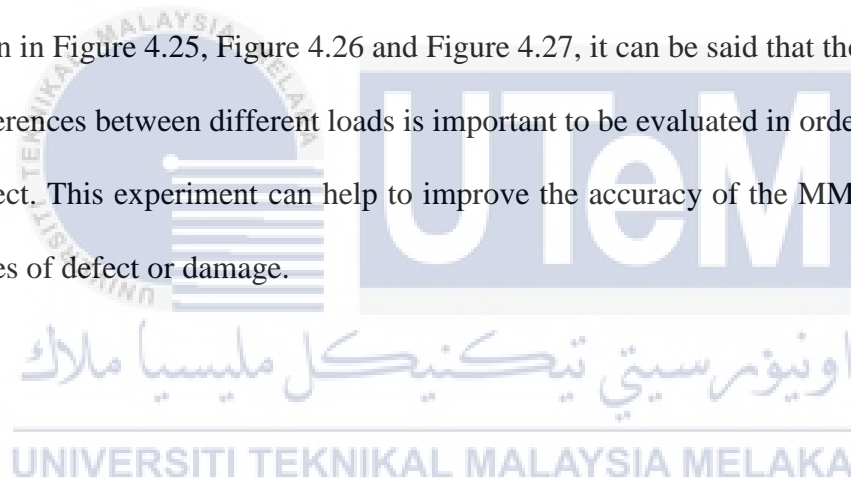
(a) Difference of tangential component for MFL

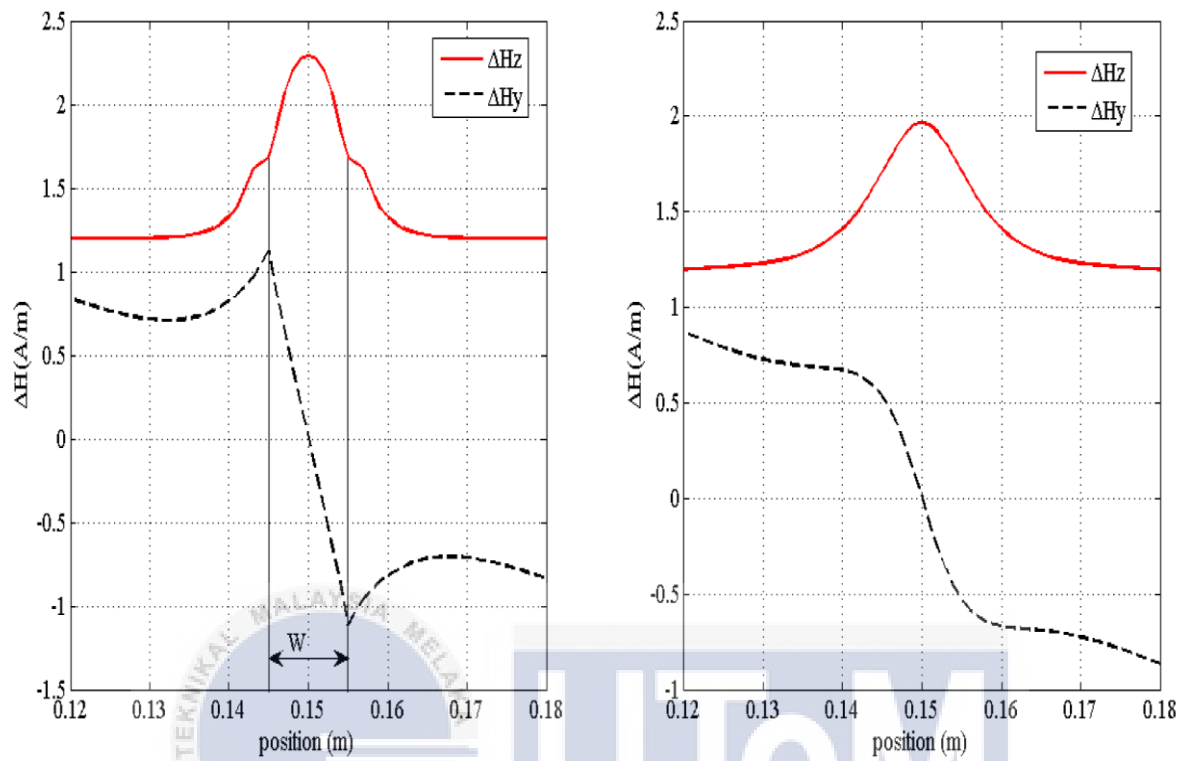
(b) Difference of normal component for MFL

Figure 4. 26 : MFL differences before and after loading (measuring line 3).

As shown in Figure 4.25, the non-smooth pattern in the area of the hole means that there is the magnetic flux disturbance caused by discontinuous material. From Figure 4.26, the curves of MFL differences along the measuring line 3 show a continuous shift in the magnetic anisotropy induced by the localized stress concentration.

Then, the MFL difference are calculated by subtracting the MFL values under 12.7 kN from 24.7 kN tensile load. The same results for measuring line 3 and 4 are obtained, as shown in Figure 4.27. Furthermore, simulations for different parameters are also applied, but the results obtained are the same except for some changes in the intensity of the MFL signals. From the results shown in Figure 4.25, Figure 4.26 and Figure 4.27, it can be said that the characteristics of MFL differences between different loads is important to be evaluated in order to classify the types of defect. This experiment can help to improve the accuracy of the MMM technique to evaluate types of defect or damage.





(d) MFL differences along measuring line 4

(b) MFL differences along measuring line 3

Figure 4. 27 : MFL differences between two tensile loads of 24.7 kN and 12.7 kN.

#### 4.3.4 FOURTH EXPERIMENT

For the fourth experiment conducted by Shengbo et al, (2016), the purpose of the experiment is to monitor fatigue cracks by using an eddy current sensor. Eddy current NDT evaluation techniques were commonly used in the inspection of structures to detect surface and near surface cracks. However, there are various type of eddy current sensors that are usually used for the inspection of the defect with no compress loading or without the evidence of fretting phenomenon.

The bolt transfers huge loading to the crack-sensitive sensor, which may lead to the failure of the sensor. To solve this problem while monitoring the crack damage, this paper proposes a smart washer to protect the transducer. A semi analytical model to monitor the damage is constructed and distributions of the electromagnetic field and eddy current field are investigated. Then, the performance of the sensor is studied.

Eddy current micro displacement sensor contains multi-layered flexible coils. Washer which is made of stainless steel, is installed to protect the sensor from huge loading while monitoring the crack as shown in Figure 4.28. The washer gives the protection to the sensor from fretting damage by transferring the load.

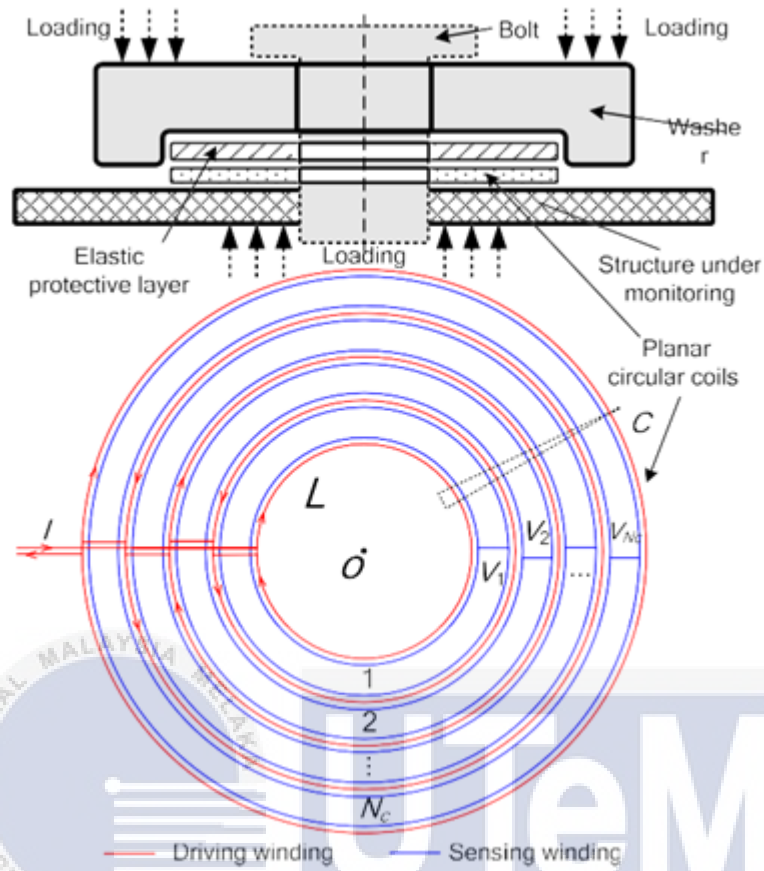


Figure 4. 28 : Geometry of the sensor and washer.

Measuring the magnetic fields can help to monitor the distribution of flaw and crack in the specimen. Two magnetic fields are produced when using the eddy current method to measure the magnetic field, which are the reaction field and the incident magnetic field from the excitation. Once the AC flows through the excitation coil, the primary magnetic field is produced and the eddy current is induced around the space and in the structure. The distribution of eddy current changed once the defect or damage is enlarged. Figure 4.29 shows the schematic view of monitoring process.

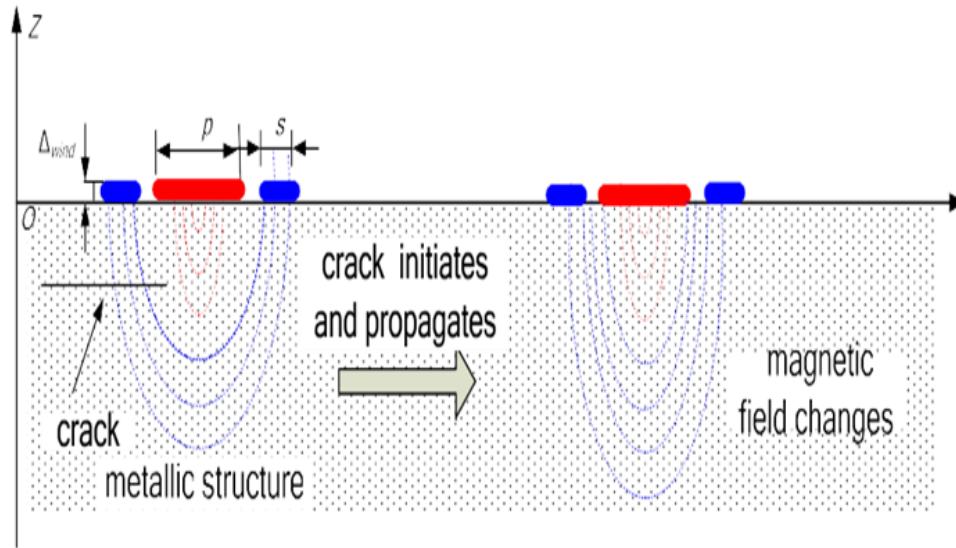


Figure 4. 29 : schematic view of monitoring process.

In an air craft body, numbers of bolt connection structures tend to expose the structures to fatigue fracture under vibration loads. This bolted connection structure is complicated to be monitored by using eddy current. A kind of protective device is used to protect the sensor because of fatigue damage and high pressure will lead the sensor from not normally functioned. For this experiment, a specialized smart washer was designed, as shown in Figure 4.30 to improve the durability and capacity of eddy current sensor bearing.

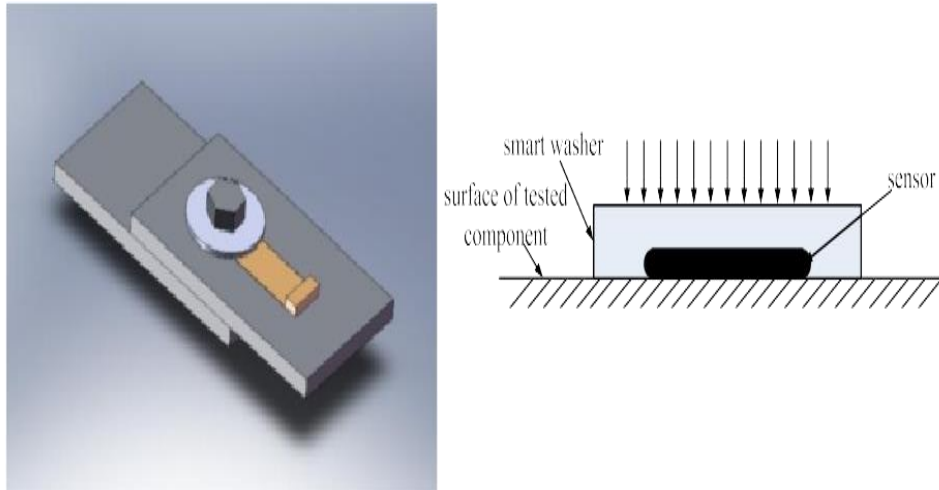


Figure 4. 30 : Smart washer

In this study, ANSYS is used to conduct the static analysis of washer, then the FEM is applied on the sensor and washer as shown in Figure 4.31. The model in Figure 4.32 is used to analyze the deformation and stress of the smart washer and sensor when subjected to the compressive force. For the smart washer, the maximum stress and maximum deformation occur at the inner edged of the groove and at the edge of the hole, respectively. However, both the maximum deformation and stress for the sensor occur at the hole edge. After that, relative radius of washer is increased from 0.5 to 0.58 and the maximum deformation and stress of the sensor is analyzed by using FEM. From Figure 4.33, maximum deformation and stress reduce when the radius increase. From the results, the deformation is  $0.01 \mu\text{m}$  and the stress is lower than 0.1 MPa when relative radius is increased to 0.85.

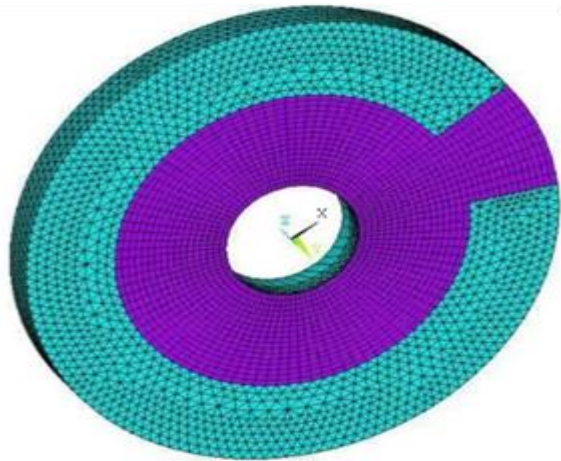
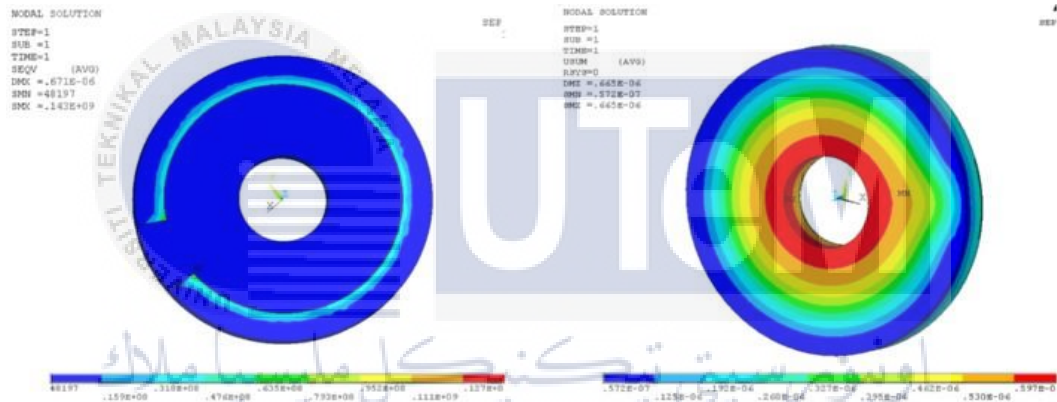
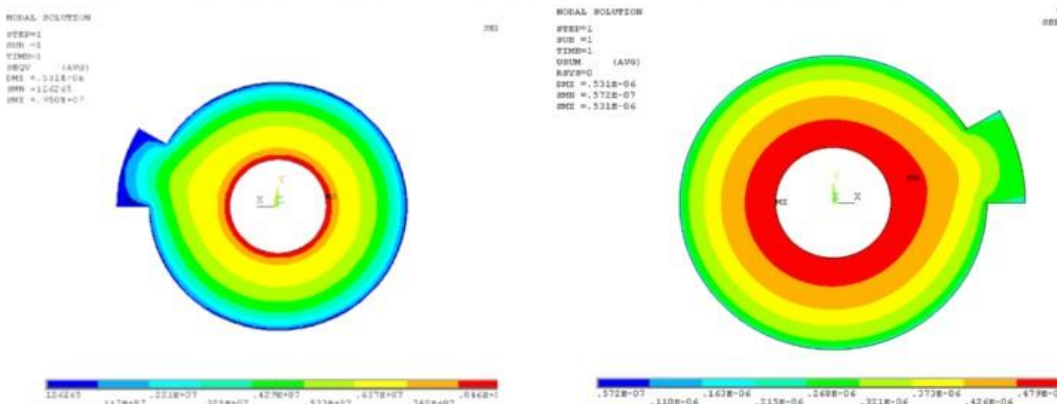


Figure 4. 31 : Finite element model.



(a) Stress distribution of the washer

(b) Deformation distribution of the washer



(c) Stress distribution of the sensor

(d) Deformation distribution of the sensor

Figure 4. 32 : Results of finite element analysis.

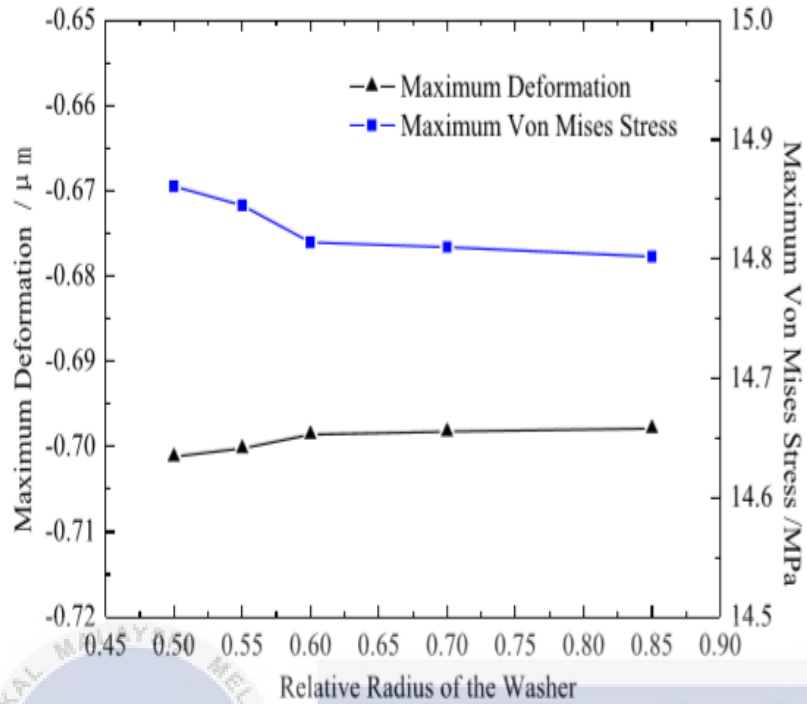


Figure 4.33 : The maximum stress and deformation with the radius of the washer.

Figure 4.34 shows the experimental setup. The Tektronix AFG3101 function generator produces a driving signal, which is amplified by the power amplifier before the coils are driven. The features of experimental setup are shown in Table 4.6. Programmed spectrums are applied using the MTS 500 material test system to implement fatigue crack initiation and propagation. The monitoring software was developed to detect the signal in real time, as shown in Figure 4.35. The four inducing signals and driving signal are displayed on the software interface. The software will post warnings when the amplitude of the inducing signals reaches a certain value.

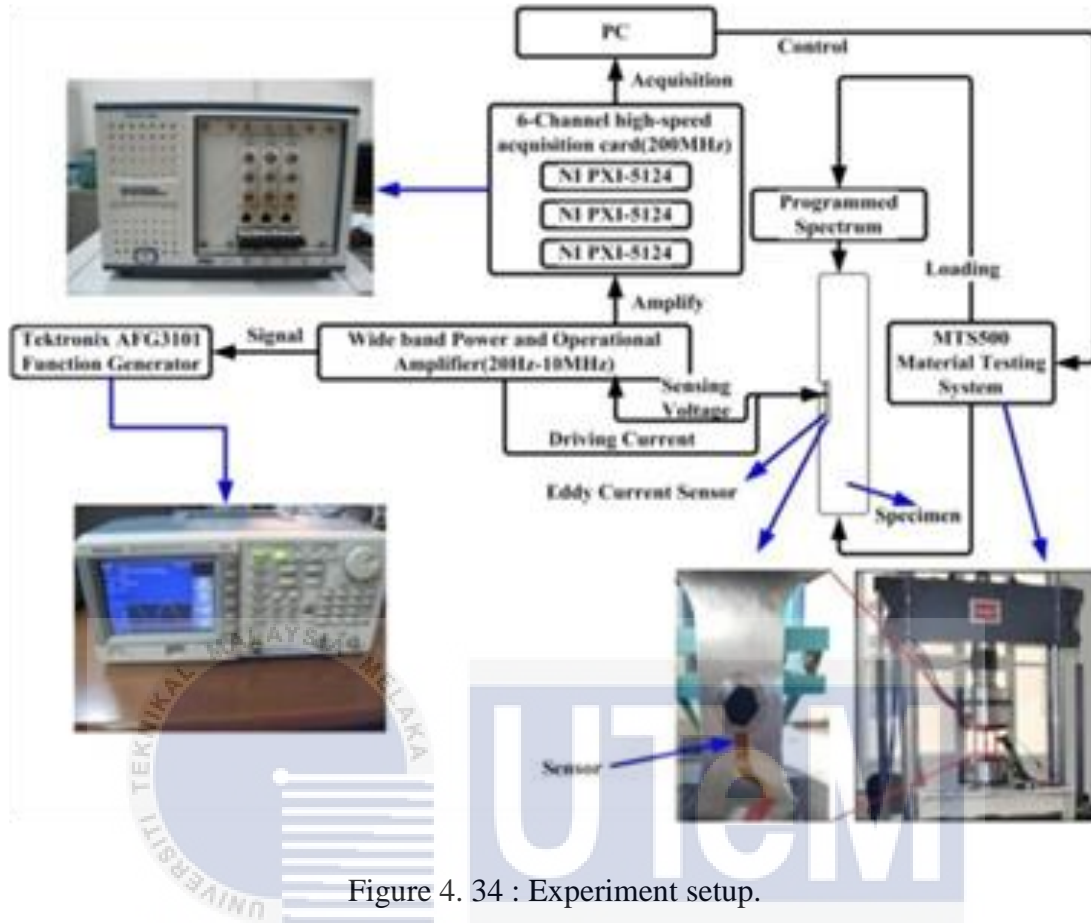


Figure 4. 34 : Experiment setup.

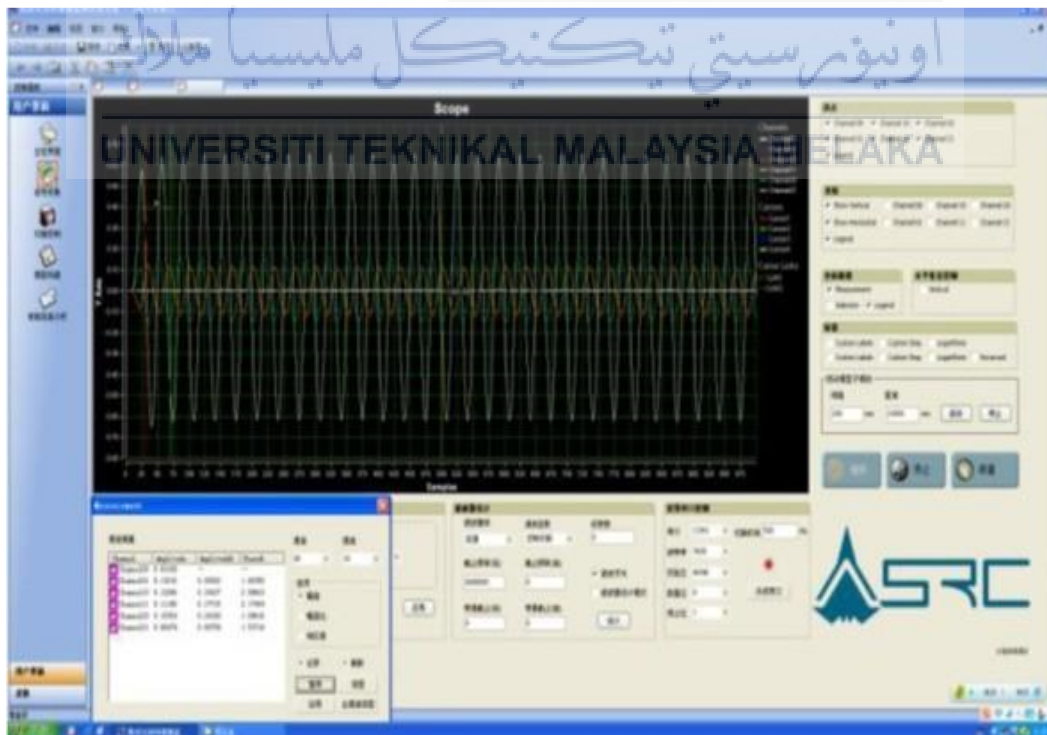


Figure 4. 35 : Self-developed monitoring software.

Table 4. 6 : Features of experiment setup.

Parameters	Description
Signal generator	$f = 0.1 \text{ Hz}-10 \text{ MHz}$ , four channels
Alternating current amplifier	10-50 dB, nominal power 15 W, optional pre-amp
Acquisition card	6 channels, up to 200 MHz sampling rate
Input	4 real-time input, external trigger, 8 control, inputs, external gate.
Output	Real-time multiplexed controller, 8, programmable control outputs.

For this experiment, 2A12-T4 aluminum is used as the specimen. This experiment consists of two groups. For the first group, the sensor is embedded into the washer which is compressed between the two dumbbell-shaped sheets while the second group is conducted in 3 % NaCl+5 % HNO<sub>3</sub> aqueous solution. Fatigue damage monitoring experiment is carried out at room temperature on an MTS 500 material test machine. The parameters are set where loading frequency  $f=15 \text{ Hz}$ , stress ratio  $R=0.06$ , maximum stress  $\sigma_{\max}=200 \text{ Mpa}$ , frequency of excitation signal is 1 MHz. Table 4.7 shows the programmed loading spectrum.

Table 4. 7 : Programmed load spectrum.

	<b>Stress level (MPa)</b>	<b>Ratio</b>	<b>Cycles</b>
Low load	150	0.06	2500
High load	200	0.06	100

The signal changes of the four sensing coils named channels 1 to 4 is as shown in Figure 4.36. From Figure 4.36, it shows that after  $2.87 \times 10^4$  loads, the first channel signal curve starts to increase. Thus, this shows that as the crack size increases, the arrayed coils detect the damage gradually. The sensing coil detects changes of the specimen at key points *A*, *B*, *C* and *D*, showing the moment when the crack first disturbs the magnetic field of each coil. With the crack extension, the crack growth rate increases with the result that load period intervals decrease by four points.

UNIVERSITI TEKNIKAL MALAYSIA MELAKA

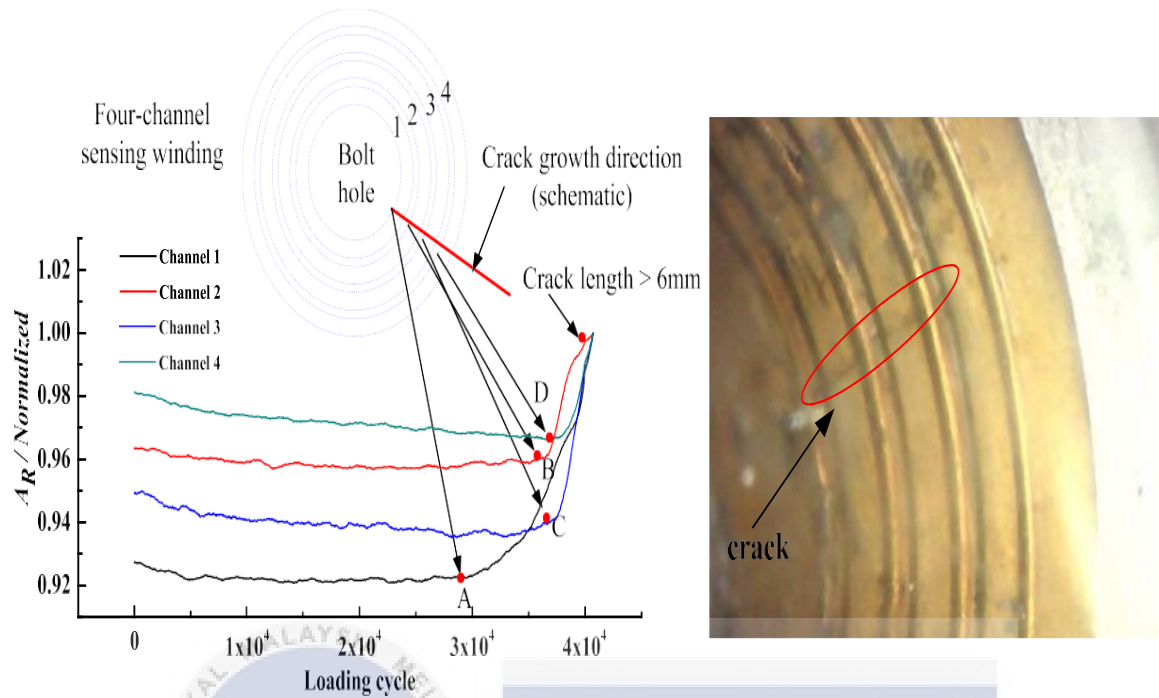


Figure 4. 36 : Changes of signals from top sensor.

A detailed study is carried out with the PXS-5 T microscope to verify the precision of the monitoring. The results are compared and listed in Table 4.8. It shows that the error is lower than 5 % except for initiation, which is caused by the distance between first coil and the sensor edge. The sensor's performance in monitoring the corrosion fatigue crack for the second group is investigated. Both the sensor and specimen are immersed in 3 % NaCl+5 % HNO<sub>3</sub> aqueous solution. The changes in signals is as shown in Figure 4.37 where the third amplitude is lower than the other one due to polyimide foil wear. For further study, the groove depth of the washer should be increased to protect the sensor.

Table 4. 8 : Comparison between the sensor's results and the analysis of fracture.

Crack length (mm)	Analysis of fracture	Monitoring result	Error (%)	Average error	Standard deviation
Initiation (0,1)	25 300	27 800	9.88	4.61 %	0.0346
1	34 400	35 090	2.00		
2	36 980	36 100	2.37		
3	38 660	37 020	4.20		

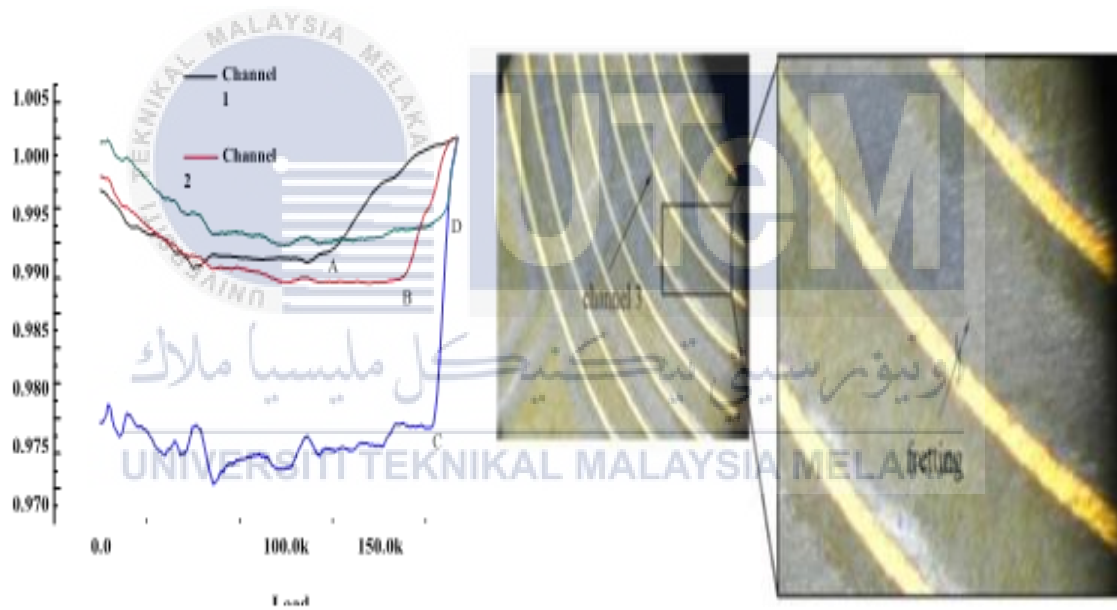


Figure 4. 37 : Changes of signal sampled by the sensor (aqueous solution).

#### 4.3.5 FIFTH EXPERIMENT

In this project Shi and Zheng, (2015) create a magnetic charge model and adapt it for 3D MMM signals modelling. The concept and theory of magnetic charge are proposed and the results of simulations of MMM signals in stress concentration zone are studied. The MMM signals that influence by a small defect is stimulated by using magnetic charge model. When the specimens act with the terrestrial magnetic field and high pressure load, the stress concentration zone will be self-magnetized. Once the load is removed, the surface self-magnetization field will reserve on strain and stress are which results in MMM signal as shown in Figure 4.38

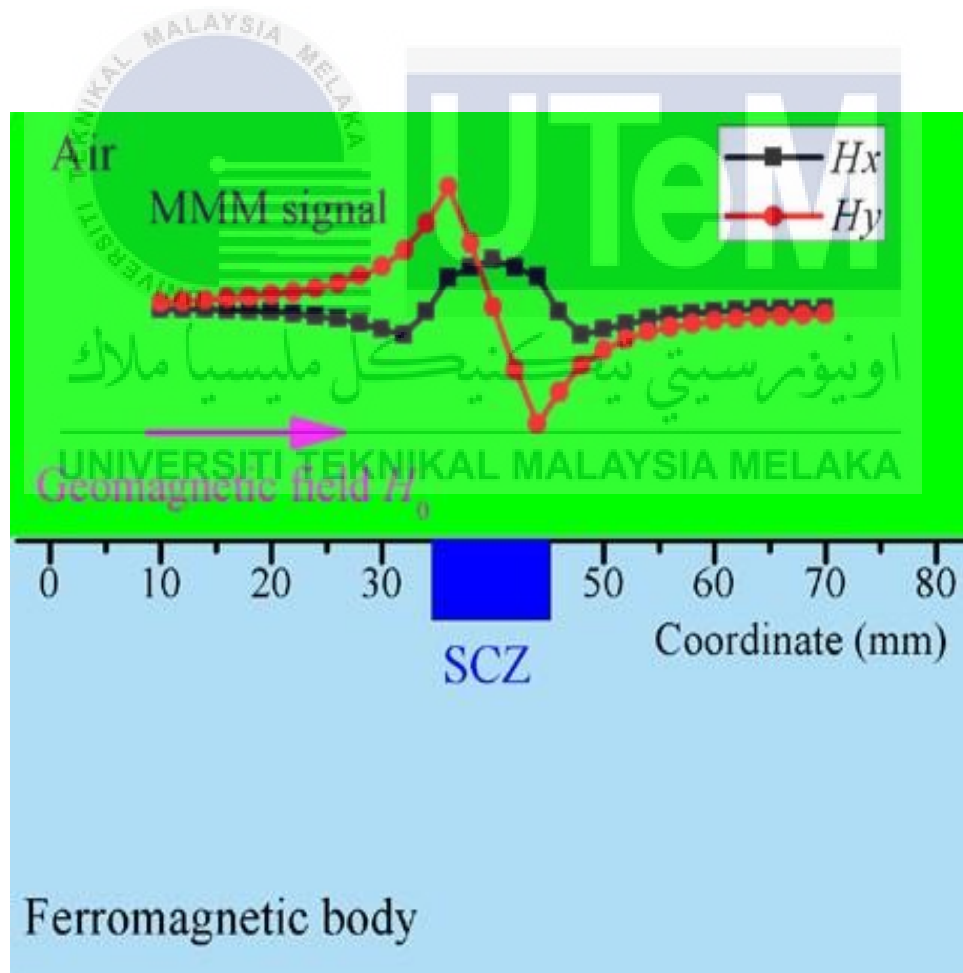


Figure 4. 38 : Schematic representation of MMM signals due to stress concentration zone.

In engineering practice, the 2D model becomes 3D model of MMM signals with the width information. During this studies, a 2D stress concentration surface model and a 3D stress concentration body model are used, as shown in Figure 4.39. Then, the 3D MMM signals are simulated.

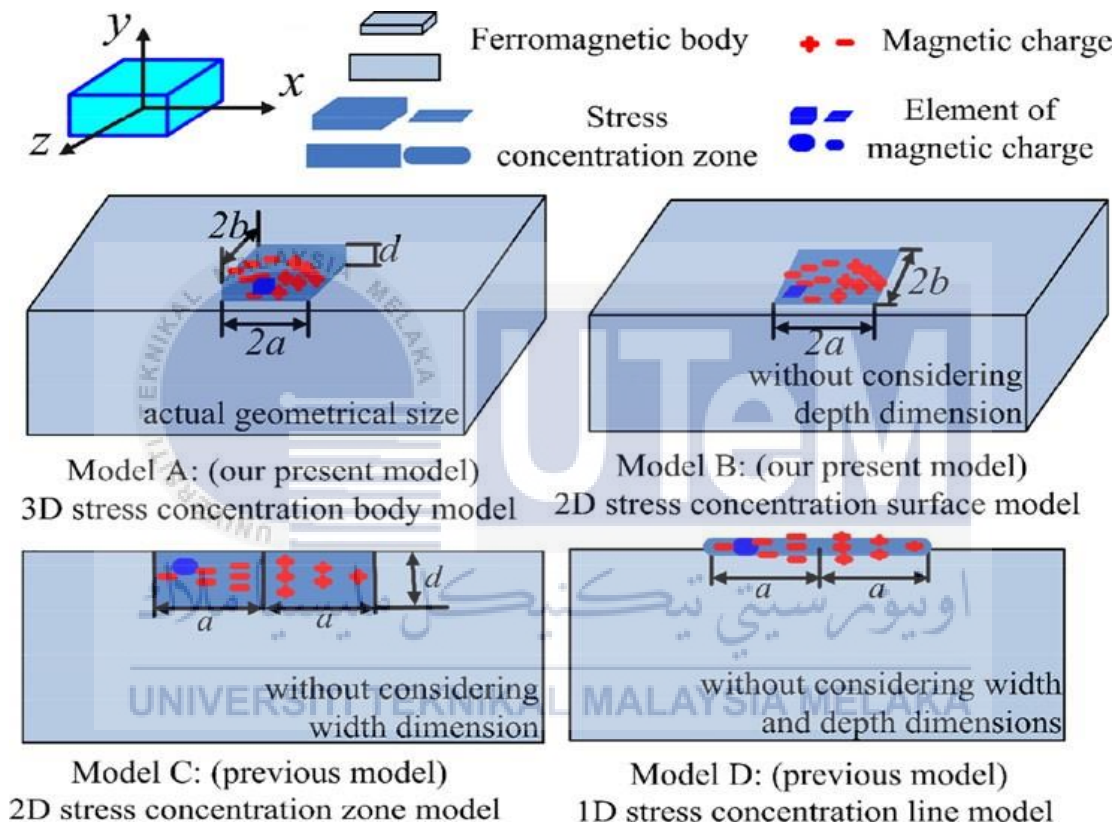


Figure 4. 39 : Magnetic charge models for the local stress concentration:

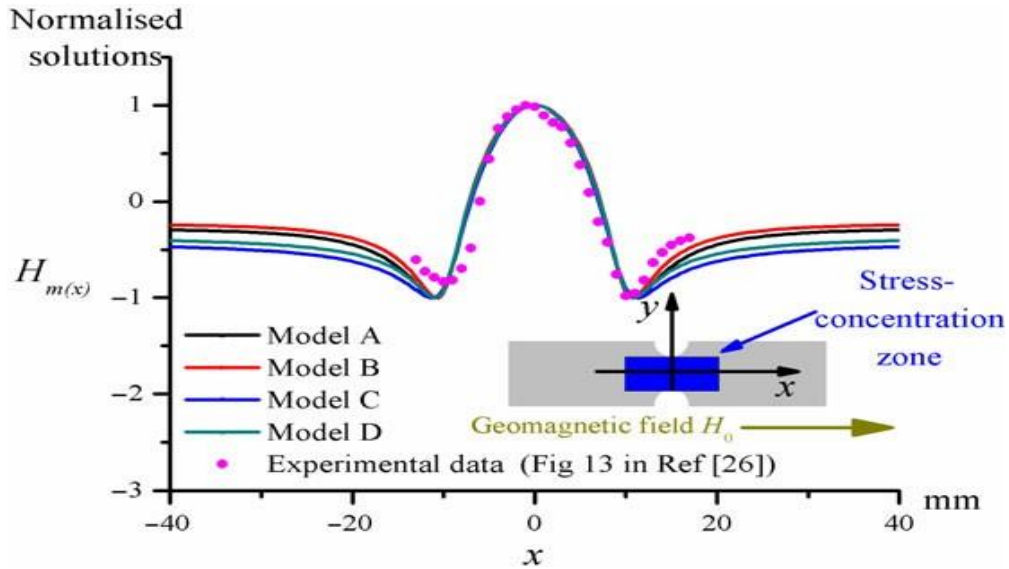


Figure 4.40 : Comparison of axial component of MMM signals between experimental data and theoretical models.

Table 4.9 : Simulations parameters for MMM simulations.

Quantity	Length $2a$	Width $2b$	Depth $d$	Lift-off $y$	Location $z$	Charge ratio $\rho_0/\rho_1$
Value	20 mm	16 mm	1 mm	2 mm	0 mm	21

Figure 4.40 shows the results obtained from the four theoretical models while Table 4.9 shows the simulation parameters used for MMM simulations. It can be said that the present models are perfectly correlate with the experimental data, for the region around the peak value and in the region close to the valley value. The purpose of this study is to utilize the MMM signals in order to solve the defect size prediction problem.

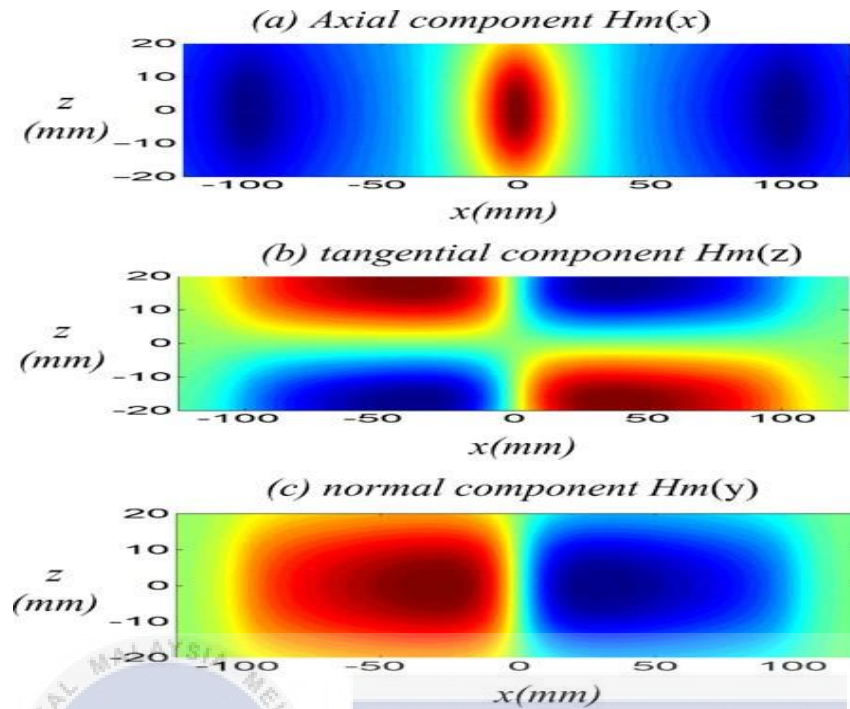


Figure 4. 41 : MMM signals simulation for a specimen with 3D stress-concentration zone.

Contour plots of the components of MMM signals in the surrounding of the stress concentration zone with  $a=100$  mm  $b=15$  mm and  $d=2$  mm and  $y= 10$  mm is shown in Figure 4.41. From the result, the polarity of the normal component changes while the axial component exhibits a peak in the maximum stress concentration. Theoretically, the MMM signal is affected by the lift-off value and the distribution of the stress concentration zone as shown in Figure 4.42. From the results obtained from Figure 4.42, it can be seen that when the length, depth or width of the stress concentration zone increase, the normal component amplitude of signals also increase. However, the amplitude of the normal component decreases when the lift-off value increases.

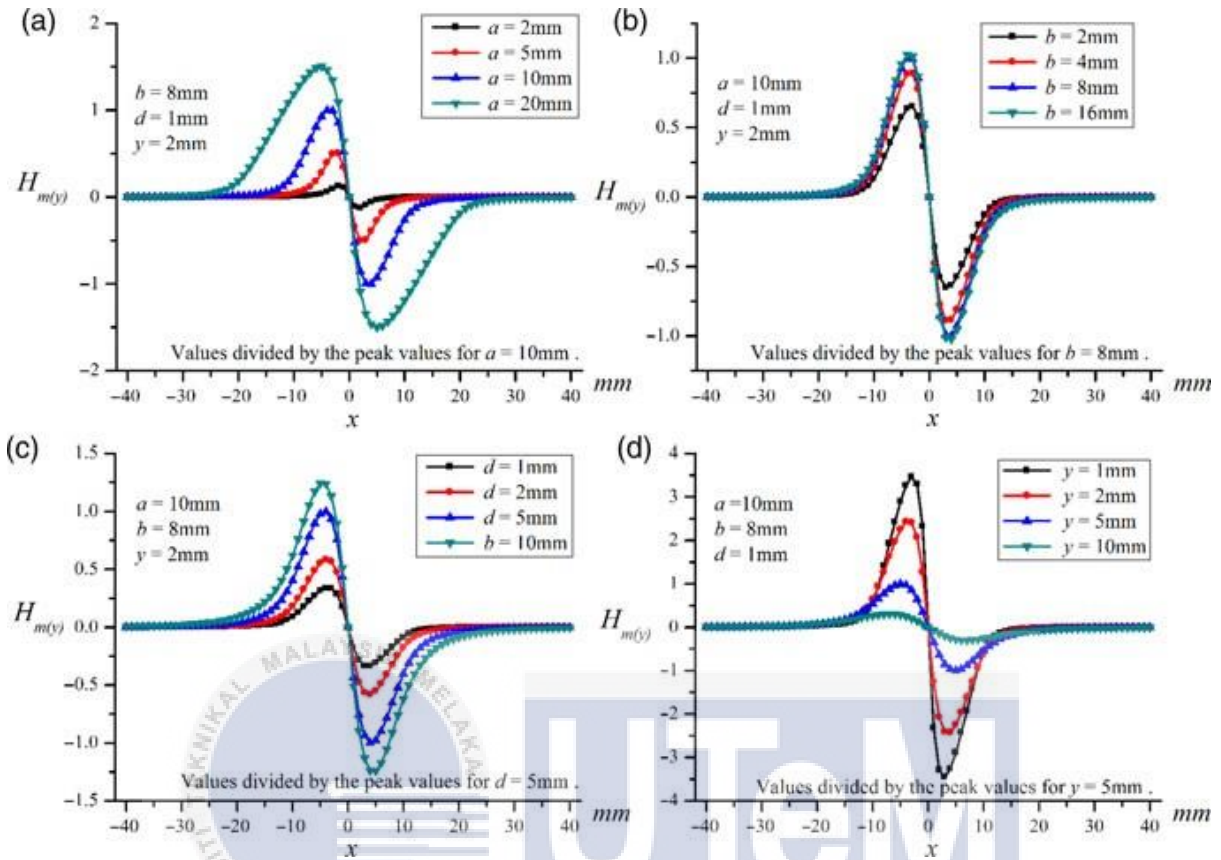


Figure 4. 42 : Distribution of normal component of MMM signals with the change in length, depth, width and lift-off values.

When a tensile force is applied along the axial axis, the specimen as shown in Figure 4.43 produces a strong stress concentration around the defect area when a tensile force is applied. The stress distribution simulated by an analytical complex variable method is shown in Figure 4.44. Based on the combination of magneto-mechanical effect and the stress analysis, the magnetic charge density distribution can be determined. Then, the magnetic field can be simulated by magnetic charge model. From the studies, it can be concluded that the magnetic charge model can be used as the MMM signal forward technique due to the similarity of simulation signals and the experimental measurements obtained from simulation example.

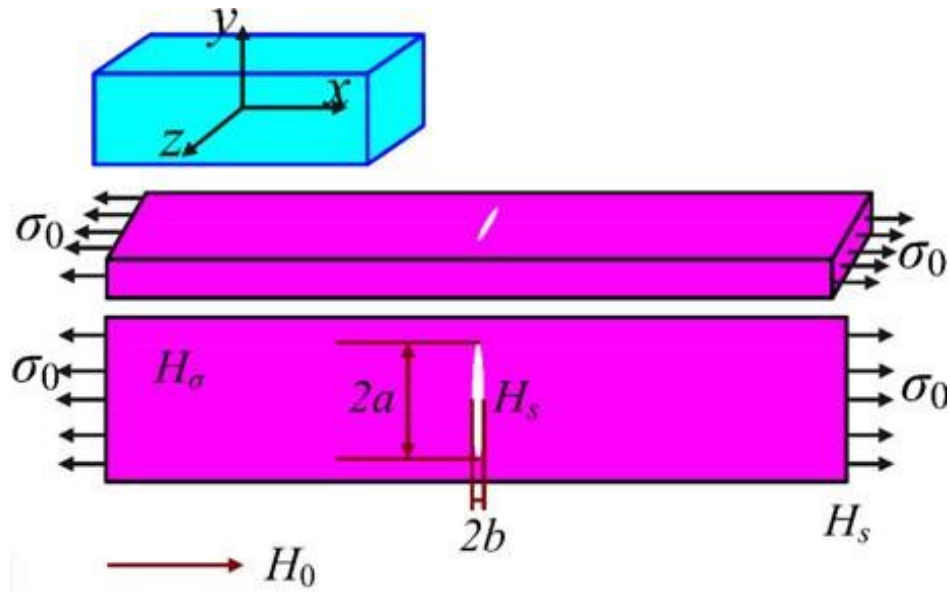


Figure 4. 43 : Specimen with a long elliptical defect.

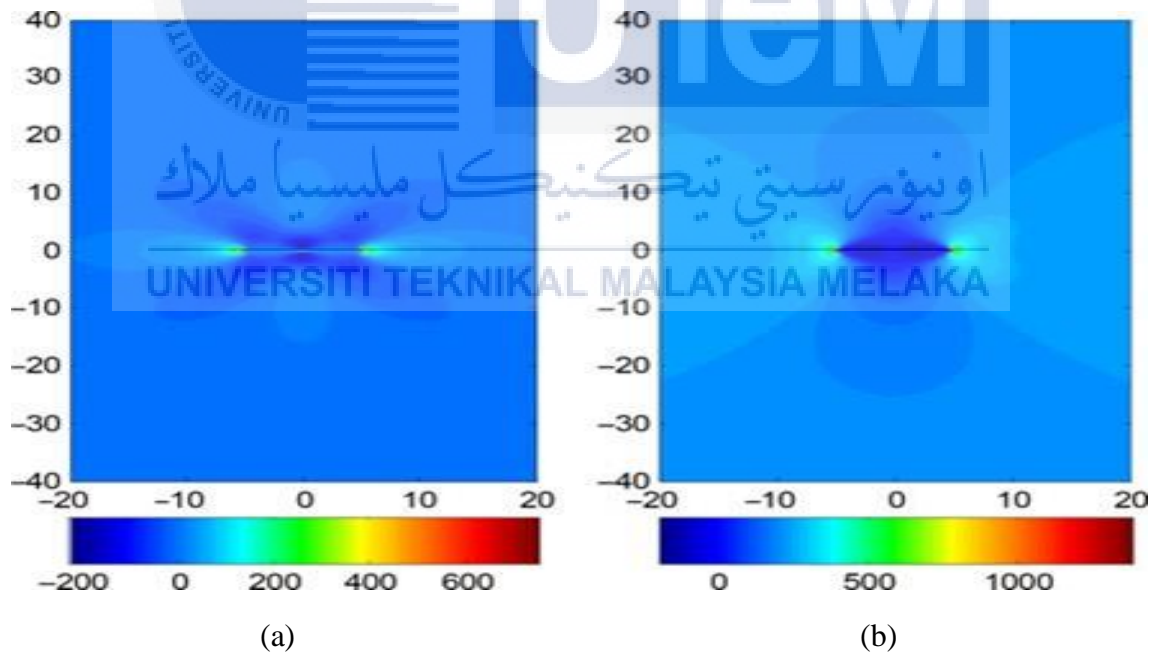


Figure 4. 44 : (a) Stress distribution in the z direction. (b) Stress distribution in the x direction.

## CHAPTER 5

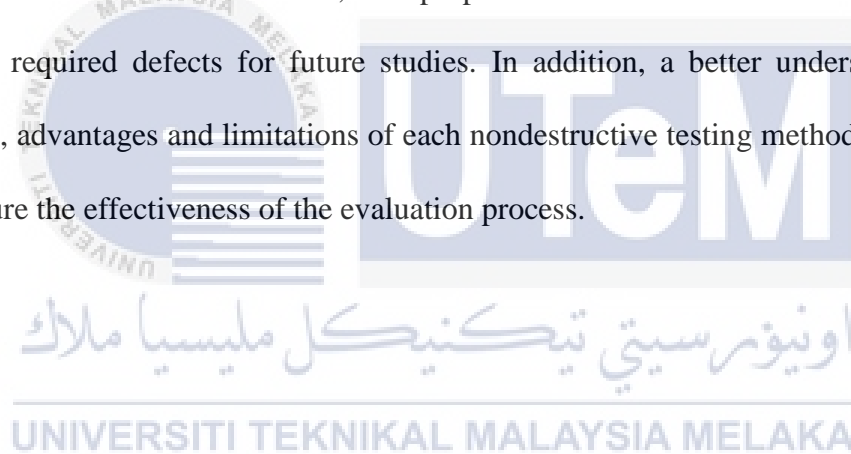
### CONCLUSION AND RECOMMENDATIONS

#### 5.1 CONCLUSION

By all counts and with proven results, it is proved that the slit parameters influence the MFL of ferromagnetic materials. From the FEA conducted on the model, it shows that the distribution of stress concentration varies with different in both slit depth and slit length parameters. In other words, the stress concentration increases when both value of slit depth and slit length increase. However, slit depth gives more influence on the distribution of stress concentration than the slit length as it is proved from the results obtained from FEA. From the results, it shows that the value of the Von Mises stress increase much higher when the depth is increased while the length of the slit is kept constant. In contrast, at the same depth with the increasing length of the slit, there are just a small increment in the value of the Von mises stress. For examples at the same length (5 mm) but with different depth, the value of the Von Mises stress increase much higher from  $1.544 \times 10^6 \text{ N/m}^2$  to  $1.724 \times 10^6 \text{ N/m}^2$  at 1 mm and 1.5 mm depth respectively. In contrast, at the same depth (1 mm) with different length of the slit, there are just a small increment in the value of the Von Misses stress which is from  $1.544 \times 10^6 \text{ N/m}^2$  to  $1.555 \times 10^6 \text{ N/m}^2$  at 5 mm and 10 mm length respectively. In addition, the results of the FEA coincident with the existed experimental results from previous researchers. The agreement between the FEA and the previous experimental results confirm that the MFL method can be used to evaluate the slit parameters of ferromagnetic materials.

## 5.2 RECOMMENDATIONS FOR FUTURE WORKS

The MMM method is a newly developed method in magnetic-based NDT. This method shows great potential because MMM is a passive method where only the earth's magnetic field is needed to obtain information of the damage that occurs in the structure. This method is basically used to determine the relationship between magnetic signal parameters in the stress concentration zone and fatigue life. However, there are still many things that need to be improved and a more detailed analysis is needed to prove this study. In many cases, combination of different NDT method is a better way to evaluate the slit parameters and to inspect the abnormalities of the structures. Hence, it is proposed to use more than one NDT method to evaluate the required defects for future studies. In addition, a better understanding of the backgrounds, advantages and limitations of each nondestructive testing method is necessary in order to ensure the effectiveness of the evaluation process.



## REFERENCES

- Ahmad, M. I. M., Ariffin, A., Abdullah, S., Jusoh, W. Z. W. & Singh, S. S. K. 2019. The probabilistic analysis of fatigue crack effect based on magnetic flux leakage. *Int. J. Reliability and Safety* 13: 18–30.
- Deng, Z., Kang, Y., Zhang, J., & Song, K. 2018. Multi-source effect in magnetizing-based eddy current testing sensor for surface crack in ferromagnetic materials. *Sensors and Actuators A: Physical*, 271, 24-36.
- Dubov, A. & Kolokolnikov, S. 2014. Application of the metal magnetic memory method for detection of defects at the initial stage of their development for prevention of failures of power engineering welded steel structures and steam turbine parts. *Welding in the World* 58 2: 225–236.
- Dubov, A. A. 1997. A study of metal properties using the method of magnetic memory 39: 401–405.
- Dubov, A. A. 2014. Energy Diagnostics - is a physical basis of the metal magnetic memory method. *11th European Conference on Non-Destructive Testing (ECNDT 2014)*, 1–8.
- Dwivedi, S. K., Vishwakarma, M., & Soni, P. 2018. Advances and Researches on Non Destructive Testing: A Review. *Materials Today: Proceedings*, 5(2), 3690-3698.
- Gupta, S. 2018. Comparison of Non-Destructive and Destructive Testing on Concrete: A Review. *Trends in Civil Engineering and Its Architecture*, 3(1).

- Ibrahim, A. & M, S. 2015. Effect of heat treatment on hardness and microstructures of AISI 1045. *Advanced Materials Research* 1119: 575–579.
- Jiao, S., Cheng, L., Li, X., Li, P., & Ding, H. 2016. Monitoring fatigue cracks of a metal structure using an eddy current sensor. *EURASIP Journal on Wireless Communications and Networking*, 2016(1).
- Pengpeng, S., & Xiaojing, Z. 2015. Magnetic charge model for 3D MMM signals. *Nondestructive Testing and Evaluation*, 31(1), 45-60.
- Sun, L., Liu, X., & Niu, H. 2019. A method for identifying geometrical defects and stress concentration zones in MMM technique. *NDT & E International*, 107, 102133.
- Shi, P., Jin, K. & Zheng, X. 2016. A general nonlinear magnetomechanical model for ferromagnetic materials under a constant weak magnetic field. *Journal of Applied Physics* 119(14).
- Shi, P., Jin, K. & Zheng, X. 2017. A magnetomechanical model for the magnetic memory method. *International Journal of Mechanical Sciences* 124–125: 229–241.
- Shi, Y., Zhang, C., Li, R., Cai, M., & Jia, G. 2015. Theory and Application of Magnetic Flux Leakage Pipeline Detection. *Sensors*, 15(12), 31036-31055.
- Usarek, Z., & Warnke, K. 2017. Inspection of Gas Pipelines Using Magnetic Flux Leakage Technology. *Advances in Materials Science*, 17(3), 37-45. doi:10.1515/adms-2017-0014.

- Verma, S. K., Bhadauria, S. S., & Akhtar, S. 2013. Review of Nondestructive Testing Methods for Condition Monitoring of Concrete Structures. *Journal of Construction Engineering, 2013*, 1-11. doi:10.1155/2013/834572.
- Wang, P., Zhu, S., Tian, G. Y., Wang, H., Wilson, J. & Wang, X. 2010. Stress measurement using magnetic Barkhausen noise and metal magnetic memory testing. *Measurement Science and Technology* 055703: 1–6.
- Wang, P., Ji, X., Yan, X., Zhu, L., Wang, H., Tian, G., & Yao, E. 2013. Investigation of temperature effect of stress detection based on Barkhausen noise. *Sensors and Actuators A: Physical, 194*, 232-239. doi:10.1016/j.sna.2013.01.027.
- Wang, Z., Gu, Y., & Wang, Y. 2012. A review of three magnetic NDT technologies. *Journal of Magnetism and Magnetic Materials, 324(4)*, 382-388.
- Wang, Z., Yao, K., Deng, B., & Ding, K. 2010. Quantitative study of metal magnetic memory signal versus local stress concentration. *NDT & E International, 43(6)*, 513-518. doi:10.1016/j.ndteint.2010.05.007.
- Yao, K., Wang, Z. D., Deng, B. & Shen, K. 2012. Experimental research on metal magnetic memory method. *Experimental Mechanics* 52: 305–314.
- Yoshimura, W., Tanaka, R., Sasayama, T., & Enpuku, K. 2018. Detection of Slit Defects on Backside of Steel Plate Using Low-Frequency Eddy-Current Testing. *IEEE Transactions on Magnetics, 54(11)*, 1-5. doi:10.1109/tmag.2018.2847729.

- Yusa, N., Chen, W., & Hashizume, H. 2016. Demonstration of probability of detection taking consideration of both the length and the depth of a flaw explicitly. *NDT & E International*, 81, 1-8.
- Yusa, N. 2009. Development of computational inversion techniques to size cracks from eddy current signals. *Nondestructive Testing and Evaluation*, 24(1-2), 39-52.
- Zhang, Y. L., Gou, R. B., Li, J. M., Shen, G. T. & Zeng, Y. J. 2012. Characteristics of metal magnetic memory signals of different steels in high cycle fatigue tests. *Fatigue and Fracture of Engineering Materials and Structures* 1–11.
- Zhang, W. 2015. Discussion on Stress Quantitative Evaluation using Metal Magnetic Memory Method. *Journal of Mechanical Engineering*, 51(8), 9. doi:10.3901/jme.2015.08.009.
- Zhong, L., Li, L., & Chen, X. 2010. Magnetic signals of stress concentration detected in different magnetic environment. *Nondestructive Testing and Evaluation*, 25(2), 161-168.

